Control Design for a Biped: Reference Trajectory Based on Driven Angles as Functions of the Undriven Angle[1]

Y. Aoustin[*], A.M. Formal'sky[**]

[*] *Institut de Recherche en Communications et Cybernétique de Nantes,*
1, rue de la Noë, BP 92101, 44321 Nantes Cedex 3, France,
E-mail: Yannick.Aoustin@irccyn.ec-nantes.fr
[**] *Institute of Mechanics of Moscow State Lomonosov University,*
1, Michurinskii pr., Moscow, 117192 Russia, E-mail: formal@imec.msu.ru
Received February 21, 2003

Abstract. This article deals with the difficult problem of developing control strategies for bipedal locomotion. We have tried to "limit" the degrees of freedom in the mechanisms and, generally, to try to account for the intermittent nature of ground impact and underactuation. We studied a planar biped consisting of five links and no feet. While walking it successively passes from a single (one leg on the ground) to a double (both legs on the ground) support phase, and it is powered only by the hip and knee joints (having no feet, the ankles are not powered). During the single support phase the biped is thus underactuated. The instantaneous double support phase can be modeled through passive impact equations. We constructed polynomial functions of the inter-link angles of the four powered articulations in relation to the angle of the supporting leg's ankle. The coefficients of these polynomials calculated for given initial, intermediate and final configurations thus defined the biped's nominal motion. Poincaré's method of analysis showed that this motion converges to a cyclic gait asymptotically. In both cases, testing two variables, torso inclination and step length, we were able to accelerate this convergence. Tracking the designed nominal trajectory was achieved through computing torque control.

Introduction

Much research [1-28] has been devoted to the control problem of a biped. Often aiming to design a control law for open-loop motions, this work has also produced several techniques for defining feedback control, specifically, through the use of reference trajectories. It is shown in [3, 13, 17] that reference trajectories can be derived from ballistic motion. Reference trajectories are generated from polynomial functions of time in [19, 23]. In [4], Van der Pol's oscillator is used to calculate them. In

[1] This work has been supported by the French Ministry for Education and Research and by GDR (the Automatic Control Research Group) of CNRS.

[5], the trajectory is adapted at each step by introducing a control for step length. Also controlling step length, [14], controlled the "zero moment point" [9] position by means of force sensors. Angular momentum information was taken into account in [8] to simulate a natural dynamic walking for a biped. It was also taken into consideration in [28] where an independent parameter known as "time scaling" is introduced. In [15], a six d.o.f. walking biped adapted to rugged terrain is developed, whereas [16, 18], the authors took an intuitive approach (based on a virtual model of the control framework) when considering the locomotion of their two planar bipedal robots. Most recently, in [25, 26], a passive motion and an optimal motion are numerically designed for a 7-link planar biped.

Other, theoretical research [1, 12, 20, 24] has been devoted to the issue of stability while walking. In [1], the authors defined the foot position of an animal or legged biped as predetermined in time and relaxed, and then, were able to introduce some control techniques suitable for stabilizing two-legged locomotion. In the last paper [24], a feedback controller for a biped is designed and the authors proved the asymptotic stability of its walking motion, using Poincaré's return map.

Our study used a five-link planar under-actuated biped without feet and our primary goal was to create a method for calculating its reference trajectory. The inter-link angles for the four actuated articulations were designed as polynomial functions, which were dependent on the angle of the non-actuated ankle articulation of the supporting leg. As long as this angle is monotonic during the swing phase, it can be used instead of time as an independent variable. Absolute time changes quite independently of the biped's displacement, whereas the ankle angle is connected to a biped's motion and thus, appeared to be a more natural independent variable. Next we computed the coefficients of the polynomials, using given initial, intermediate and final configurations and certain conditions. The biped configuration was therefore expressed by polynomials, for each ankle angle value. In this manner, our under-actuated system became a set with the same number of actuators and degrees of freedom. The polynomials defined the biped's nominal motion (reference trajectory) and it was found to have cyclic gait. Applying the Poincaré return map method, we were able to show the asymptotic stability of this cyclic gait. Two factors were tested (changing the trunk inclination and step length) and both were found to accelerate convergence to the cycle. Finally, we were able to track the designed nominal (reference) trajectory, using computed torque control. In this work we have used a planar biped model with no feet. However, we think that these methods can be extended to more complex models.

The paper is organized as follows. A dynamical model of the biped is presented in Section 1. In Subsection 1.1, the swing motion equations are presented, as are the passive impact equations in Subsection 1.2. Section 2 covers the reference trajectories for the inter-link actuated angles. Gait is

described in Subsection 2.1. The choice of the inter-link angles as polynomial functions of the non-actuated ankle angle is elaborated in Subsection 2.2. A way of designing a simpler model of swing motion is proposed in Subsection 2.3. Section 3 is devoted to the problem of designing a periodic gait regime. In Subsection 3.1, we present a methodology for designing periodic gait and in Subsection 3.2 we look at this from a numerical point of view. Section 4 is dedicated to the analysis of the asymptotic stability of the periodic gait. In Subsection 4.1, we apply the Poincaré map method to show that this cyclic gait is asymptotically stable. Adjusting torso orientation as a way of accelerating convergence to the cyclic gait is studied in Subsection 4.2. Adjusting step length is studied in Subsection 4.3. Section 5 deals with problems encountered tracking the reference trajectory and in Section 6 we briefly evaluate some acceptable perturbations. Finally, Section 7 is devoted to our conclusion and reflections as to future research.

1. Dynamical Model of the Biped

To construct a dynamical model, first, we will generate the motion equations for the single support and the instantaneous double support phases inherent to locomotion. Impact equations for the double support phase will also be presented and finally, all these equations will be written in matrix form.

1.1 Swing Motion Equations

Our biped walks in a vertical $x\,y$ sagittal plane. The biped mechanism is composed of a trunk and two identical double-link legs (Fig. 1). Let us introduce vector $X=(x,y,\delta_1,\delta_2,\delta_3,\delta_4,\alpha)^*$ with seven generalized coordinates (star * means transposition). It is defined by the two coordinates *x, y* of the trunk mass center, and the five orientation angles $(\delta_1,\delta_2,\delta_3,\delta_4,\alpha)^*=q$ of the legs and the trunk (Fig. 1, left). The angles are defined as positive for counter clockwise motion. Vector *q* shall be known as the "configuration vector" or "a configuration". The vector of the inter-link angles $\delta=(\delta_1,\delta_2,\delta_3,\delta_4)^*$ represents the "figure" vector. Thus, $q=(\delta^*,\alpha)^*$. These variables allow us to describe the single support, double support and supportless phases.

All links are assumed massive and rigid. All joints are revolute and ideal, which means that the effect of friction in the joints is neglected. Let the vector $\Gamma=(\Gamma_1,\Gamma_2,\Gamma_3,\Gamma_4)^*$ denotes the torques applied in the hip and knee joints. Let $R_1(R_{1x},R_{1y})$ and $R_2(R_{2x},R_{2y})$ be the forces applied to the leg tips (Fig. 1, right). The motion equations of the biped in the swing phase have the following well-known form:

$$A(q)\ddot{X}+H(q,\dot{q})=D\Gamma+D_j(q)R_j \qquad (1.1)$$

$$D_j^*(q)\ddot{X} + H_j(q,\dot{q}) = 0 \qquad (1.2)$$

Here $A(q)$ is the symmetric, positive definite 7×7 matrix of kinetic energy; $H(q,\dot{q})$ is the 7×1 vector of the centrifugal, Coriolis and gravity forces; D is a 7×4 fixed matrix, consisting of zeros and units; $D_j(q)$ is a 7×2 matrix; $H_j(q,\dot{q})$ is a 2×1 matrix (all these matrices are described in Appendix *1*); j denotes the supporting (i.e., stance) leg ($j=1$ or 2). System (1.1) can usually be represented by a set of scalar nonlinear differential equations using a 14×1 state vector. However, in the context of this paper it is not useful. Setting a condition of a contact between the supporting leg tip and the ground implies that both the abscise and ordinate of that leg tip do not change. Matrix equation (1.2) represents the second derivative of the corresponding relations and shows that the acceleration of the stance leg tip is zero. Thus, matrix equation (1.2) means that the supporting leg tip does not move. A passive ball joint models the contact between the stance leg tip and the ground. However, during locomotion, the ground surface does not exercise any adhesive nor attractive forces on the stance leg tip. For this reason the vertical component of the ground reaction must be directed upwards. We will verify this requirement during the computations.

Our biped has five degrees of freedom in the swing phase, but four actuators only; thus, it is under-actuated in the single support phase.

1.2 Passive Impact Equations

Walking consists of alternating single and double support phases. We shall assume that the double support phase is instantaneous and model it through passive impact equations. An impact appears at a time $t=T$, for this time the swing leg touches the ground. We shall assume that the impact is passive, absolutely inelastic, and that the legs do not slip. Given these conditions, the ground reactions can be considered impulsive forces and defined by Dirac delta-functions [3]:

$R_j = I_{R_j}\Delta(t-T)$ *(j=1, or 2)*

Here $I_{R_j}(I_{R_{xj}}, I_{R_{yj}})$ is the vector of the magnitudes of the impulsive reaction in the swing (before an impact) leg j.

Impact equations can be obtained through integration of the matrix motion equation (1.1) for the infinitesimal time from *T-0* to *T+0* of instantaneous impact. The torques supplied by the actuators at the joints, the centrifugal, Coriolis and gravity forces have finite values, thus they do not influence an impact. Consequently the impact equations can be written in the following matrix form:

$$A(q(T))(\dot{X}^+ - \dot{X}^-) = D_k(q(T))I_{R_k}, \quad k \neq j \qquad (1.3)$$

Here *q(T)* denotes the configuration of the biped at instant *t=T* (this configuration does not change at the instant of the double support), $\dot{X}^-$ and $\dot{X}^+$ are respectively the velocity vectors just before and just after an impact. The velocity of the supporting leg tip before an impact equals to zero,

$$D_j^*(q(T))\dot{X}^- = 0 \tag{1.4}$$

The swing leg k after an impact becomes the supporting leg. Therefore, its tip velocity becomes zero after an impact,

$$D_k^*(q(T))\dot{X}^+ = 0 \tag{1.5}$$

Generally speaking, two results are possible after an impact. The rear leg will take off the ground or both legs will remain on the ground. In the first case, the vertical component of the velocity of the taking-off leg tip just after an impact must be directed upwards; we shall also assume that there is no interaction between the taking-off leg tip and the ground *i.e.*, $I_{R_j} = 0$. In the second case, the rear leg tip velocity has to be zero just after an impact. Since passive leg tips are used, the ground will produce the impulsive forces (generally, $I_{R_1} \neq 0$, $I_{R_2} \neq 0$) and this implies that the vertical component of the impulsive ground reaction in the rear leg (as in the fore leg) is directed upwards. For the second case, we have the following matrix equations:

$$A(q(T))(\dot{X}^+ - \dot{X}^-) = D_1(q(T))I_{R_1} + D_2(q(T))I_{R_2},\ D_1^*(q(T))\dot{X}^+ = 0,\ D_2^*(q(T))\dot{X}^+ = 0$$

This system consists of *11* scalar equations and contains *11* unknown variables that form the vectors $\dot{X}^+$, I_{R_1}, I_{R_2}. In general, the result of a passive impact is dependent on two factors: the biped's configuration at the instant of an impact and the direction of the fore leg tip velocity just before impact [3]. Equations (1.3) and (1.5) are suitable for the first case only when the rear leg takes off the ground. We checked the two possible results after an impact and only the first result occurs: the rear leg rises after an impact.

Linear system (1.3), (1.5) has a unique solution $\dot{X}^+$, I_{R_j}, because its corresponding matrix is non-singular (this assertion is proved in Appendix *2*).

System (1.3) - (1.5) consists of *11* scalar equations. Excluding *6* scalar variables: $\dot{x}^-$, $\dot{y}^-$, $\dot{x}^+$, $\dot{y}^+$, $I_{R_{xk}}$ and $I_{R_{yk}}$ from this system, we obtain the following linear relation between the vectors $\dot{q}^-$ and $\dot{q}^+$ of the angular velocities just before and just after the impact [3]:

$$\dot{q}^+ = J(q(T))\dot{q}^- \tag{1.6}$$

The matrix *J(q(T))* depends only on the biped configuration *q* at instant *T* of double support.

2. Reference Trajectory For Inter-Link Angles

In several works (see, for example, [19, 23]), polynomial functions of time were used to design a nominal walking regime (reference trajectory) of a biped. In other words, each driven inter-link angle δ_ℓ (ℓ = *1, ..., 4*), was given as a polynomial function of time. However, in our biped model ankle angle α is undriven and, because of disturbances the transferring leg may touch the ground before the prescribed time. Should this happen a configuration error will arise at the beginning of the next half step. To avoid this error, each driven inter-link angle δ_ℓ will be defined for our model as a function of α.

2.1 Description of the Gait

Legs *1* and *2* of the biped swap their roles from one half step to the other (see Fig. 2). The transferring leg is shown in Fig. 2 by dotted lines. We suppose that leg *1*, moving forward, touches the ground with an inelastic impact and does not slip. Leg *2* loses contact with the ground and rises. The legs assume a symmetrical role from one half step to the next one.

From a prescribed initial configuration, we are interested in moving the biped through the swing phase into a prescribed final configuration. In both boundary configurations, the two legs are on the ground. Thus, the two boundary configurations are equal to the two double support configurations.

Let $t = 0$ be the initial time and $t = T$ be the final time for a single support motion. If the boundary configurations of the swing phase are given, then angles α_i and α_f are prescribed. The indices *i* and *f* shall respectively correspond to initial (at $t = 0$), and final (at $t = T$) configurations of the biped.

2.2 Polynomial Functions for Inter-Link Angles

We now will express inter-link angles δ_ℓ (ℓ = *1, ..., 4*) for the four actuated articulations as polynomial functions of the stance leg's tibia angle α, relative to the vertical axis. In several experiments (see, for example, [13, 19]) and in our biped simulations, this angle α changes strictly monotonically during the single support motion (Fig. 3 confirms this property in our system). Therefore, it is possible to use angle α instead of time *t* as an independent variable for these polynomials. Unlike absolute time, which changes independently of the biped's displacement, the ankle angle α is connected to the biped's behavior and thus appears to be a natural independent variable. We believe this variable will be more adaptable than absolute time to take into account the influence of perturbations affecting the biped. Our reference trajectory gains the geometric

expression $\delta_\ell = \delta_\ell(\alpha)$ (ℓ = *1, ..., 4*), which is to say that the biped reference trajectory is calculated in function of angle α (not time).

We want to obtain a desired final figure of the biped before an impact. Therefore, the segment $\left[\alpha_i, \alpha_f\right]$ is divided into two parts $\left[\alpha_i, \alpha^\circ\right]$ and $\left[\alpha^\circ, \alpha_f\right]$. Angles δ_ℓ (ℓ = *1, ..., 4*) are defined as a fifth order polynomials of angle α in the first segment:

$$\delta_\ell(\alpha) = a_{\ell 0} + a_{\ell 1}\alpha + a_{\ell 2}\alpha^2 + a_{\ell 3}\alpha^3 + a_{\ell 4}\alpha^4 + a_{\ell 5}\alpha^5 \qquad \alpha_i \le \alpha \le \alpha^\circ \tag{2.1}$$

The first and second time derivatives of these four polynomial functions $\delta_\ell(\alpha)$ are defined such that,

$$\dot{\delta}_\ell(\alpha) = \delta'_\ell(\alpha)\dot{\alpha}, \quad \ddot{\delta}_\ell(\alpha) = \delta'_\ell(\alpha)\ddot{\alpha} + \delta''_\ell(\alpha)\dot{\alpha}^2 \tag{2.2}$$

with ‘ representing the derivation with respect to the variable α.

Let us suppose that in the second segment $\left[\alpha^\circ, \alpha_f\right]$ the inter-link joint angles do not change and the whole mechanism turns around point *S* (see Fig. 1) like a rigid body, until it hits the bearing surface:

$$\delta_\ell(\alpha) \equiv \delta_\ell(\alpha^\circ) = \delta_\ell(\alpha_f) = const, \qquad \alpha^\circ \le \alpha \le \alpha_f \tag{2.3}$$

Maintaining figure δ constant before impact helps to reduce the error in the biped configuration at the beginning of the next step [13, 19]. Without such a constraint, the biped configuration at the end of the single support phase can be altered from the desired configuration, (due to an error in the measured angle α for example). The absolute angular velocities of all five links in the segment $\left[\alpha^\circ, \alpha_f\right]$ equal to $\dot{\alpha}$.

Let $\dot{\delta}_\ell(\alpha^\circ) = \ddot{\delta}_\ell(\alpha^\circ) = 0$, then it follows from (2.2) that

$$\delta'_\ell(\alpha^\circ) = 0, \quad \delta''_\ell(\alpha^\circ) = 0 \text{ and } (\ell = 1, ..., 4), \tag{2.4}$$

as long as $\dot{\alpha} \neq 0$ when $\alpha = \alpha^\circ$.

Given the equalities (2.4), the functions $\ddot{\delta}_\ell(\alpha)$ and consequently the torques in the joints change continuously over time, and this, as long as, the derivative $\ddot{\alpha}$ also changes continuously.

At the instant when $\alpha = \alpha_{int} = (\alpha_i + \alpha^\circ)/2$ we shall call the configuration *intermediate*.

Let us specify the initial, intermediate, and final configurations as well as the initial angular velocities. Thus the values

$$\alpha_i, \quad \alpha_f, \quad \dot{\alpha}_i, \quad \delta_\ell(\alpha_i), \quad \dot{\delta}_\ell(\alpha_i), \quad \delta_\ell(\alpha_{int}), \quad \delta_\ell(\alpha_f) \qquad (\ell = 1, ..., 4) \tag{2.5}$$

are defined.

All six coefficients for each fifth order polynomial function $\delta_\ell(\alpha)$, (ℓ = *1, ..., 4*) (2.1) can be calculated, using the four values, $\delta_\ell(\alpha_i)$, $\dot{\delta}_\ell(\alpha_i)/\dot{\alpha}_i$, $\delta_\ell(\alpha_{int})$, $\delta_\ell(\alpha_f)$ from (2.5) and two conditions (2.4). In fact, we do not need the velocities $\dot{\alpha}_i$, $\dot{\delta}_\ell(\alpha_i)$ separately to calculate the coefficients of the polynomials. We only need to know the ratios $\dot{\delta}_\ell(\alpha_i)/\dot{\alpha}_i = \dfrac{\partial\delta_\ell(\alpha_i)}{\partial\alpha}$. Note that polynomials (2.1) can also be formulated if $\alpha^\circ = \alpha_f$.

If, before an impact, the biped mechanism rotates like a rigid body (δ=*const*), the velocity of the fore leg tip is directed vertically downwards. The resulting vertical component of the impulsive ground reaction applied to the fore leg tip at the instant of an impact will be directed upwards. This assertion is clear from a physical point of view. It is analytically proven in Appendix *3*.

2.3 A Way to Design Swing Motion

The figure vector $\delta(\alpha)$ can be calculated, if the values in (2.5) are known. In this case, a semi-inverse problem occurs with respect to the single support motion design, because part of coordinates (inter-link angles) are given as functions of angle α, whereas angle α can be calculated only from motion equations.

Single support motion can be defined by integrating the equations (1.1), (1.2). However, in our study we have used a simpler method.

Let σ denote the angular momentum around the motionless ankle joint *S*. Momentum σ is the linear combination of the angular velocities $\dot{\delta}_\ell$, (ℓ = *1, ..., 4*) and $\dot{\alpha}$, and has the coefficients $f_\ell(\delta)$ (ℓ = *1, ..., 5*), which are known functions of the figure vector δ and the biped parameters

$$\sigma = \sum_{\ell=1}^{4} f_\ell(\delta)\dot{\delta}_\ell + f_5(\delta)\dot{\alpha} \tag{2.6}$$

Function $f_5(\delta)$ describes the biped's total moment of inertia around the motionless ankle joint *S* and $f_5(\delta) > 0$ for all figures δ.

If $\delta = \delta(\alpha)$ and consequently $\dot{\delta}(\alpha) = \delta'(\alpha)\dot{\alpha}$, then

$$\sigma = f(\alpha)\dot{\alpha} \tag{2.7}$$

Function $f(\alpha)$ is given by

$$f(\alpha) = \sum_{\ell=1}^{4} f_\ell[\delta(\alpha)]\delta'_\ell(\alpha) + f_5[\delta(\alpha)] \tag{2.8}$$

Function (2.8) depends on the biped parameters and on the coefficients of polynomials (2.1). Let us note that $f(\alpha) \equiv f_5(\delta) \equiv constant$ in segment $\left[\alpha^{\circ}, \alpha_f\right]$, where the figure δ of the biped does not change. This *constant* is the total inertia moment of the mechanism around joint *S* and is not equal to zero.

A simple differential equation follows from equality (2.7):

$$\dot{\alpha} = \sigma / f(\alpha) \tag{2.9}$$

Ankle joint S is passive and there is no driven torque acting in it. Gravity is the only force creating external torque in it, therefore, the angular momentum changes according to the equation:

$$\dot{\sigma} = -Mg\left[x_C(\delta,\alpha) - x_S\right] \tag{2.10}$$

Here M is the total biped mass, g the acceleration due to gravity, $x_C(\delta,\alpha)$ the abscissa of the biped mass center (which depends on figure δ and ankle angle α), x_S is the constant abscissa of point *S*. However, if $\delta = \delta(\alpha)$ is a known vector-function, then we come to the following equation:

$$\dot{\sigma} = -Mg\left[x_C(\alpha) - x_S\right] \tag{2.11}$$

and the biped mass center abscissa $x_C(\alpha)$ is a known function of angle α.

Instead of equations (1.1), (1.2), the second order system (2.9), (2.11) is used here to design swing motion. The initial value σ for this system can be calculated from formula (2.7), when initial values α_i and $\dot{\alpha}_i$ are known. We then calculate the solutions of system (2.9), (2.11) numerically, assuming that a solution exists and is unique over the given time interval. After solving the system (2.9), (2.11) the joint torques Γ_ℓ (ℓ = *1, ..., 4*) can be found from equations (1.1), (1.2).

System (2.9), (2.11) follows also from (1.1), (1.2) of course. Furthermore, a parallel can be drawn with the concept of the zero-dynamics [29]. The dynamics of α are in fact the internal dynamics of the biped when the applied control is such that the desired reference trajectory of variables δ_ℓ, (ℓ = *1, ..., 4*) are tracked perfectly.

If angle α changes strictly monotonically over time, then we obtain from system (2.9), (2.11) the following first order equation:

$$\frac{d\sigma^2}{d\alpha} = -2Mg\left[x_C(\alpha) - x_S\right] f(\alpha)$$

It follows from this equation that

$$\sigma^2(\alpha) - \sigma^2(\alpha_i) = F(\alpha),\ F(\alpha) = -2Mg\int_{\alpha_i}^{\alpha}\left[x_C(\nu) - x_S\right] f(\nu)\,d\nu$$

and (see (2.7))

$$\sigma^2(\alpha_f)-\sigma^2(\alpha_i)=f^2(\alpha_f)\dot{\alpha}_f^2-f^2(\alpha_i)\dot{\alpha}_i^2=F(\alpha_f) \tag{2.12}$$

3. Periodic Regime

In this section we will describe the cyclic gait of the biped, for the case when the double support configurations are the same. This situation appears, for example, when a biped is walking on a planar surface.

3.1 A Way to Design Periodic Gait

The initial and final configurations of the single support motion are the same, but the legs are swapped. Therefore, given the inter-link angles and ankle angle α (see (2.5) and Fig. 4) the following equalities should be true:

$$\delta_1(\alpha_i)=\delta_4(\alpha_f),\quad \delta_2(\alpha_i)=\delta_2(\alpha_f)-\delta_3(\alpha_f),\quad \delta_3(\alpha_i)=-\delta_3(\alpha_f),\quad \delta_4(\alpha_i)=\delta_1(\alpha_f)$$

$$\alpha_f=\alpha_i-\delta_1(\alpha_i)+\delta_3(\alpha_i)+\delta_4(\alpha_i) \tag{3.1}$$

Before an impact, $\dot{\delta}=0$. Thus, we can consider angular velocity $\dot{\alpha}^-$ of the biped just before an impact (that is final velocity $\dot{\alpha}_f$ of the single support motion) as a unique input parameter for the impact matrix equation (1.6). If value $\dot{\alpha}_f$ is given, then, using the prescribed terminal configuration, we can algebraically determine all five angular velocities just after impact using system (1.6). These velocities $\dot{\alpha}_i$, $\dot{\delta}_\ell(\alpha_i)$, ($\ell$ = *1, ..., 4*) also are those of the beginning of the next swing phase. So, using the prescribed initial, intermediate and terminal configurations, we can find polynomials (2.1), and then, using equations (2.9), (2.11), the single support motion. At the end of this motion we calculate a new angular velocity $\dot{\alpha}_f$, *etc*.

Applying system (1.6) we can establish the linear relation between the terminal velocity (or $\dot{\alpha}^-$) and the initial velocity $\dot{\alpha}_i$ (or $\dot{\alpha}^+$)

$$\dot{\alpha}_i=h\dot{\alpha}_f\quad (\text{or } \dot{\alpha}^+=h\dot{\alpha}^-),\quad \dot{\alpha}_f=h^{-1}\dot{\alpha}_i=s\dot{\alpha}_i\quad (\dot{\alpha}^-=h^{-1}\dot{\alpha}^+=s\dot{\alpha}^+) \tag{3.2}$$

Here, *h* depends on the biped configuration at time *T*: $h=h(\alpha_f)\neq 0$.

We shall call u_n, velocity $\dot{\alpha}_i$ (or $\dot{\alpha}^+$) at the start of half step number *n*. Using expressions (2.12) and (3.2), we can obtain the next value u_{n+1}, which is the initial velocity $\dot{\alpha}_i$ for half step number *n+1*.

$$f^2(\alpha_f)s^2u_{n+1}^2-f^2(\alpha_i)u_n^2=F(\alpha_f) \tag{3.3}$$

Formula (3.3) gives the relation between values u_n and u_{n+1}

$$u_{n+1} = p(u_n) \quad \text{or} \quad u_{n+1} = \left[\frac{F(\alpha_f) + f^2(\alpha_i) u_n^2}{f^2(\alpha_f) s^2} \right]^{1/2} \tag{3.4}$$

Thus, function (3.4) represents the evolution of the biped angular velocity $\dot{\alpha}_i$ from one half step to another. Using this expression (3.4), we can construct in plane (u_n, u_{n+1}) the Poincaré return map [30].

Let u_e be the *equilibrium* point of transformation (3.4) – the fixed point of mapping (3.4). This point is defined by the following equalities

$$u_e = p(u_e) \text{ or } u_e = \left[\frac{F(\alpha_f)}{f^2(\alpha_f) s^2 - f^2(\alpha_i)} \right]^{1/2} \tag{3.5}$$

Thus, as in [27], we can conclude that a unique equilibrium u_e exists, if and only if $F(\alpha_f)\left[f^2(\alpha_f) s^2 - f^2(\alpha_i) \right] > 0$.

The value u_e yields a cyclic motion, which for us is the desired gait.

Using the same method, it is possible to analyze the case, when $\alpha^\circ = \alpha_f$. To obtain a more robust configuration tracking we defined a non-zero interval $\left[\alpha^\circ, \alpha_f \right]$ with conditions (2.3). (Yes, dear Yannick, it was previously reference to formula (2.4), (i.e. (10)), but in my opinion reference to formula (2.3) is better. Ah! In this case OK, Dear Alexander, it is better)

3.2 Numerical Design of Periodic Gait

Here, we will consider RABBIT's parameters [21, 23]. The lengths of the femurs and the tibias are equal: *0.4 m*. However, their masses are different: *8 kg*, for the femur and *6 kg* for the tibia. The length of the trunk is *0.625 m* and its mass equals *20 kg*.

Let the following angles (in radians) be for the initial, intermediate and final configurations:

$$\alpha_i = 0.1571, \quad \alpha_f = -0.3840, \quad \alpha^\circ = -0.3389, \quad \delta_1(\alpha_{int}) = 2.9285, \quad \delta_2(\alpha_{int}) = 2.9322$$

$$\delta_3(\alpha_{int}) = 0.2722, \quad \delta_4(\alpha_{int}) = 2.3996, \quad \delta_2(\alpha_i) = 2.6704, \quad \delta_2(\alpha_f) = 3.2114 \tag{3.6}$$

$$\delta_1(\alpha_i) = \delta_4(\alpha_i) = \delta_1(\alpha_f) = \delta_4(\alpha_f) = 2.9147, \quad \delta_3(\alpha_i) = -\delta_3(\alpha_f) = -0.5411$$

These three configurations are represented by Fig. 2. Expressions (2.1), (2.3) for functions $\delta_\ell(\alpha)$ $(\ell = 1,...,4)$ were designed with parameters (3.6). These functions $\delta_\ell(\alpha)$ $(\ell = 1,...,4)$ are shown in Fig. 4. The graphs of functions $\delta_\ell(\alpha)$ have a horizontal element because of conditions (2.3).

Using expressions (3.5), we calculated the cyclic regime for the configurations in (3.6) given above. The angular velocity u_e and the corresponding time T_e of the cyclic motion are the following

$$u_e = \dot{\alpha}_i = -1.4124 s^{-1}, \quad T_e = 0.5337\ s \tag{3.7}$$

The curves in Fig. 3 and Fig. 5 present respectively the evolution over time of angle α and of the actuated joint angles δ_ℓ $(\ell = 1, ..., 4)$, for the found cyclic gait. In accordance with the conditions (2.3), the curves of the actuated joint angles δ_ℓ become horizontal at the end of the swing phase. Angle α decreases in a strictly monotonic manner during swing motion. A stick diagram of the cyclic walking is presented in Fig. 6. ψ is the angle between the trunk and the horizontal axis. Fig. 7 shows the cyclic gait in planes (α,σ), $(\psi,\dot{\psi})$. The curve in plane (α,σ) is not closed, because α is the angle between the tibia of the supporting leg and the vertical axis, and the legs swap their roles from one half step to the next. The curve in plane $(\psi,\dot{\psi})$ is of course closed. The torques $\Gamma_\ell(t)$ $(\ell = 1, ..., 4)$ for this cyclic gait are computed too. We have designed also the values of the actuator angular velocities versus the torque values (using four gear actuator ratios equal to 50). These values are compatible with RABBIT's actuator characteristics [21, 23]. The numerical solution of equations (1.1), (1.2) shows that the swing leg tip moves over the ground during the single support of the cyclic gait (see Fig. 6), and the vertical component of the ground reaction in the stance leg is directed upward. It follows from the solution of impact equations (1.3), (1.5) that after an impact, the vertical velocity component of the rear leg tip is directed upwards, consequently, the rear leg rises.

4. Stability of the Cycle and Acceleration of the Convergence

In this section we will perform a numerical analysis with the Poincaré map to show that the cycle constructed previously, is asymptotically orbitally stable with respect to nominal motion. Our desired gait on a planar surface is periodic. In order to accelerate the convergence to the desired cyclic gait we will test two strategies: varying the trunk inclination or the step length from one half step to the next. As a result of speeding up the convergence to the cycle, our biped's behavior will become more reactive.

4.1 Stability of the Periodic Gait

Using the numerically constructed graph of function (3.4) shown in Fig. 8, we can find its intersection with the quadrant bisector and we name this the equilibrium point u_e ($-1.4124\ s^{-1}$, see (3.7)) for periodic motion and thus, verify whether this motion is stable. The point u_e in the Poincaré map in Fig. 8 is asymptotically stable. However, when the initial velocity $\dot{\alpha}_i$ surpasses $-1.05\ s^{-1}$, the angular velocity $\dot{\alpha}$ becomes positive during the swing motion. Then, the angle α increases and the biped moves back to its initial configuration. This means that the absolute value of the initial angular momentum is not sufficiently large. When $\dot{\alpha}_i < -2.75\ s^{-1}$, the vertical component of the ground reaction in the supporting leg becomes zero and the biped loses contact with the ground. This fact can be established, using equations (1.1), (1.2). For the walking locomotion it is impossible to have the supporting leg rise, thus, the attraction region of the equilibrium point in the Poincaré map is

$$-2.75\ s^{-1} < \dot{\alpha}_i < -1.05\ s^{-1} \tag{4.1}$$

The equilibrium u_e is asymptotically stable point of transformation (3.4). Appendix *4* shows that the cyclic motion of the biped corresponding to this point is asymptotically stable as well.

As displayed in Fig. 8, the transitional process converges to the point (u_e, u_e) monotonically, but "slowly", because the curve of function (3.4) is "close" to the bisector of the quadrant.

Let us assume that either the current biped's configuration or its angular velocities at the start of the swing phase do not coincide with desired one. To correct this, we compute the polynomials to connect both the current initial configuration and the velocities, with the desired terminal configuration. In this manner, the biped configuration becomes desired one to the end of the single support. Afterwards, the motion converges to the desired periodic gait asymptotically.

4.2 Acceleration of the Convergence to the Cycle by Correction of the Torso Orientation

In an effort to accelerate the convergence to a cyclic regime, first, we use a parameter defined by the angle $\delta_2(\alpha_f)$, which is equal to the inclination of the trunk at the end of the swing phase. Then, we will vary this parameter from one half step to the next half step in function of the initial angular velocity u_n and the initial trunk inclination $\delta_2(\alpha_i)$.

Let us denote by ξ_n the angle of the torso inclination $\delta_2(\alpha_i)$ at the start of half step number *n*, and by v_n the angle of the torso inclination $\delta_2(\alpha_f)$ at the end of the same half step. The following relation exits between ξ_n and v_{n-1} (see the second expression of (3.1))

$\xi_n = v_{n-1} - \delta_3(\alpha_f)$

because at the instant of impact, the biped configuration does not change. However the legs exchange their role after an impact, but δ_2 remains the angle between the *supporting* leg and the trunk. We assume here that $\delta_3(\alpha_f) = const$ during the walking.

We now want to see what influence varying the initial and final torso inclinations will have on parameter u_{n+1}. Let us consider the following function instead of function (3.4):

$$u_{n+1} = f(u_n, \xi_n, v_n) = q(u_n, v_{n-1}, v_n) \tag{4.2}$$

If variables v_{n-1} and v_n are equal to their nominal values $v_{n-1} = v_n = v_e = 3.2114$ (see (3.6)), then functions (3.4) and (4.2) coincide i.e., $q(u_n, v_e, v_e) \equiv p(u_n)$. The curve of this function is presented in Fig. 8. The curve of function (4.2) is constructed numerically in Fig. 9, with $u_n = u_e = -1.4124\ s^{-1} = const$ (see (3.7)) and $v_n = v_e = 3.2114 = const$. The curve of function (4.2) is constructed in Fig. 10, with $u_n = u_e = -1.4124\ s^{-1} = const$ and $v_{n-1} = v_e = 3.2114$. So, the curves $u_{n+1} = q(u_e, v_{n-1}, v_e)$ and $u_{n+1} = q(u_e, v_e, v_n)$ are shown in Fig. 9 and Fig. 10 respectively.

Our numerical investigations show that when $v_{n-1} > 3.7$ ($\delta_2(\alpha_i) > 3.159$), the angular variable α first decreases and then, in the middle of the half step, starts to increase, but never reaches the given value α°. The angular momentum σ and velocity $\dot{\alpha}$, which were negative, both become positive. The biped initially moves forward, and then back to its initial configuration. When $v_{n-1} < 2.23$ ($\delta_2(\alpha_i) < 1.69$), function $f(\alpha)$ becomes zero for a certain value α after the beginning of the step. If $f(\alpha)$ attains 0, the angular velocity $\dot{\alpha}$ tends to $-\infty$. This means that solving system (2.9), (2.11) can not be prolonged after the instant when $\dot{\alpha}$ becomes $-\infty$. The inequality $\delta_2(\alpha_i) < 1.69$ indicates that initially the trunk is leaning far too forward. When this is the case and because of functions (2.1), (2.3), (2.4) with the indicated values $\delta_2(\alpha_i)$, the biped cannot take a step.

Fig. 9 and Fig. 10 show that the trunk inclinations v_{n-1} and v_n influence the velocity u_{n+1}. The curves in the Fig. 8 – Fig. 10 allow us to formulate a linear approximation of the function (4.2) in a domain around the equilibrium point (u_e, v_e, v_e),

$$\Delta u_{n+1} = a\Delta u_n + b\Delta v_{n-1} + c\Delta v_n \quad (\Delta u_n = u_n - u_e,\ \Delta v_{n-1} = v_{n-1} - v_e,\ \Delta v_n = v_n - v_e) \tag{4.3}$$

Fig. 8 produces the value $a = 0.70$; Fig. 9, the value $b = 0.80\ s^{-1}$; Fig. 10, the value $c = 0.577 s^{-1}$. (Note that a is smaller than one.)

Now we will try to accelerate the convergence, using the following linear corrector:

$$\Delta v_n = d\Delta u_n + g\Delta v_{n-1} \quad (v_n = v_e + d(u_n - u_e) + g(v_{n-1} - v_e)) \tag{4.4}$$

We will calculate constant values for feedback gains *d* and *g*. Relation (4.4) shows that the desired trunk inclination at the end of the swing phase needs to be changed. The new final trunk inclination is a linear function of the deviations of the velocity $\dot{\alpha}_i$ and the trunk inclination $\delta_2(\alpha_i)$ at the start of the same swing phase. Therefore the polynomial function $\delta_2(\alpha)$ changes at each step with a new initial value, a new final value and a new ratio $\dot{\delta}_2(\alpha_i)/\dot{\alpha}_i$, while the intermediate value $\delta_2(\alpha_{int})$ does not.

We can consider (4.3), (4.4) as a system of difference equations. This system can be reduced to the following difference equation

$$\Delta u_{n+2} - (a + cd + g)\Delta u_{n+1} + (ag - bd)\Delta u_n = 0 \tag{4.5}$$

Let us choose the coefficients *d* and *g* of the corrector to satisfy the following algebraic equations

$$cd + g + a = 0, \quad ag - bd = 0$$

Solving these equations relative to the gains *d* and *g*, we obtain the formulas:

$$d = -a^2/(ac + b), \quad g = -ab/(ac + b) \tag{4.6}$$

Using the coefficients in (4.6), the eigenvalues of the difference equation (4.5) (or of system (4.3), (4.4)) become equal to zero and solving this equation two steps beyond any of the initial conditions produces a solution zero. It is obvious that both deviations Δu_n and Δv_n become zero after two steps. Using the values *a*, *b*, *c*, given above, we find from (4.6) the feedback gains of $d = -0.4\ s$, and $g = -0.4652$. Substituting expression (4.4) into formula (4.2), we obtain the following nonlinear transformation:

$$u_{n+1} = q\left[u_n,\ v_{n-1},\ v_e + d(u_n - u_e) + g(v_{n-1} - v_e)\right] \tag{4.7}$$

Let the initial conditions be the following: $u_0 = -1.7\ s^{-1}$ and $v_0 = v_e = 3.2114$. The two piecewise constant curves obtained under these conditions in plane (n, u_n) are shown in Fig. 11. The first curve presents the transitional process described by function (3.4) without any corrector. The second curve presents the transitional process described by function (4.7) with a corrector (4.4). The transitional process converges to the equilibrium u_e much faster with a corrector. Thus, the torso orientation is an efficient parameter for controlling the biped's motion.

The attraction region of the equilibrium point for the system with a corrector (4.4) is the following:

$$-1.73\ s^{-1} < \dot{\alpha}_i < -1.05\ s^{-1} \tag{4.8}$$

This region is smaller than the attraction region for the system without a corrector (see inequalities (4.1) in Section 4.1). The lower limitation is due to the fact that the vertical component of the ground reaction becomes null.

In our study, we used a dead-beat corrector (the poles are at the origin) with coefficients (4.6) to demonstrate the idea of convergence acceleration. It would, of course, be possible to apply a different corrector.

4.3 Acceleration of the Convergence to the Cycle by Correction of the Step Length

Here we are going to try to speed up the convergence to the cyclic regime, using the parameter $\delta_3(\alpha_f)$, the angle between the femurs. Angle $\delta_2(\alpha_f)$ will remain constant during all the walking phases. And if angles $\delta_1(\alpha_f)$, $\delta_4(\alpha_f)$ are also kept constant, angle $\delta_3(\alpha_f)$ is directly dependent on step length.

Let us denote by ζ_n the angle $\delta_3(\alpha_i)$ between the femurs at the start of half step number *n,* and, by w_n, the angle $\delta_3(\alpha_f)$ between the femurs at the end of the same half step. This gives us the following relation between ζ_n and w_{n-1} (see the third expression of (3.1))

$$\zeta_n = -w_{n-1},$$

because during the impact, the biped configuration does not change. The biped's legs do change their role after an impact, but angle δ_3 is measured from the *supporting* leg. As we did when adjusting torso inclination, we will now look at what happens to parameter u_{n+1} when the initial and final step lengths are varied. To start we will take a function similar to (4.2):

$$u_{n+1} = \varphi(u_n, \zeta_n, w_n) = r(u_n, w_{n-1}, w_n) \qquad (4.9)$$

If variables w_{n-1} and w_n are equal to their nominal values $w_{n-1} = w_n = w_e = 0.5411$ (see (3.6)), then functions (3.4) and (4.9) coincide, *i.e.*: $r(u_n, w_e, w_e) \equiv p(u_n)$. This function is presented graphically in Fig. 8. Function (4.9) with $u_n = u_e = -1.4124\ s^{-1} = const$ (see (3.7)) and $w_n = w_e = 0.5411 = const$, (reducing to $u_{n+1} = r(u_e, w_{n-1}, w_e)$) is constructed numerically in Fig. 12. Function (4.9) with $u_n = u_e = -1.4124\ s^{-1} = const$ and $w_{n-1} = w_e = 0.5411$ (reducing to $u_{n+1} = r(u_e, w_e, w_n)$) is shown graphically in Fig. 13. Fig. 12 and Fig. 13 clearly display the influence of step length on the velocity u_{n+1}.

The curves in Fig. 8, Fig. 12 and Fig. 13 allow us to design a linear approximation of function (4.9) in a domain around the equilibrium point (u_e, w_e, w_e) similar to approximation (4.3)

$$\Delta u_{n+1} = a\Delta u_n + b\Delta w_{n-1} + c\Delta w_n \quad (\Delta u_n = u_n - u_e,\ \Delta w_{n-1} = w_{n-1} - w_e,\ \Delta w_n = w_n - w_e) \tag{4.10}$$

The values $a = 0.70$ (see above), $b = -0.1522\ s^{-1}$ and $c = -2.70\ s^{-1}$ can be calculated using Fig. 8, Fig. 12, and Fig. 13 respectively.

Now we can speed up the convergence using a linear corrector similar to (4.4):

$$\Delta w_n = d\Delta u_n + g\Delta w_{n-1} \quad (w_n = w_e + d(u_n - u_e) + g(w_{n-1} - w_e)) \tag{4.11}$$

where the feedback gains *d* and *g* have constant values. Relation (4.11) implies that we change the desired step length at the end of each swing phase. The new step length is a linear function of the deviations in velocity $\dot{\alpha}_i$ and pace length $\delta_3(\alpha_i)$, at the start of the same swing phase. The polynomial function $\delta_3(\alpha)$ changes at each step, taking on a new initial value, a new final value and a new ratio $\dot{\delta}_3(\alpha_i)/\dot{\alpha}_i$, while the intermediate value $\delta_3(\alpha_{int})$ remains unchanged.

System (4.10), (4.11) of difference equations can be reduced to one difference equation similar to (4.5). Using the values *a*, *b*, *c*, calculated above and computing the feedback gains *d* and *g* in accordance to formulas (4.6), we find $d = 0.2196\ s$, $g = -0.052$. Substituting expression (4.11) into formula (4.9), we obtain the following nonlinear transformation:

$$u_{n+1} = q\left[u_n,\ w_{n-1},\ w_e + d(u_n - u_e) + g(w_{n-1} - w_e)\right] \tag{4.12}$$

If we set the following initial conditions, $u_0 = -1.7\ s^{-1}$ and $w_0 = w_e = 0.5411$, the two piecewise constant curves generated in plane $(n,\ u_n)$ can be seen in Fig. 14. The first curve presents the transitional process described by function (3.4) without a corrector. The second curve presents the transitional process described by function (4.12) with a corrector (4.11). We can note that when the corrector is applied, the transitional process converges more rapidly to equilibrium u_e. Thus, as in the case of the torso inclination corrector where results were similar, we can see that step length is an efficient parameter for controlling the biped's motion.

The attraction region of the equilibrium point for the system with a corrector (4.11) is the following:

$$-2.1\ s^{-1} < \dot{\alpha}_i < -1.05\ s^{-1} \tag{4.13}$$

This region is slightly smaller than the attraction region for the system without a corrector (see inequalities (4.1) in Section 4.1).

5. Tracking of the Reference Trajectory

Our five-link footless biped (see Fig. 1) in the swing phase is a mechanism with five degrees of freedom (as long as contact between the support and stance leg tip is modeled as a pivot). The five independent angles δ_1, δ_2, δ_3, δ_4, α can be used to describe its motion. If we exclude the ground reaction applied to the stance leg tip from the system (1.1), (1.2), we can describe the single support motion phase with a system of five scalar differential equations, each of a second order. This system can be written in the following well-known matrix form:

$$B(\delta)\ddot{q} + K(q,\dot{q}) = E\Gamma \qquad (5.1)$$

Here $B(\delta)$ is a 5×5 symmetric matrix; $K(q,\dot{q})$ is a 5×1 vector; E is a 5×4 fixed rank 4 matrix consisting of zeros and units.

We can present system (5.1) in the following way: the first four scalar motion equations contain the inter-link control torques; the fifth scalar equation, expressing the angular momentum theorem, does not contain these torques. It contains only the torque of gravity force. Thus, it is possible to express system (5.1) so that $E = \left\| \begin{matrix} E_4 \\ 0 \end{matrix} \right\|$. Here E_4 is a 4×4 non-singular matrix.

The angular momentum σ is described by expression (2.6). If $\delta = \delta(\alpha)$ is the given vector-function, then the momentum σ can be expressed by equation (2.7) with the function $f(\alpha)$ given in formula (2.8). If $f(\alpha) \neq 0$ in segment $\left[\alpha_i, \alpha^\circ\right]$, then differentiating expression (2.9), we can calculate the second derivative $\ddot{\alpha}$

$$\ddot{\alpha} = \frac{d}{dt}\left(\frac{\sigma}{f(\alpha)}\right) = \frac{\dot{\sigma} f(\alpha) - \sigma \dot{f}(\alpha)}{f^2(\alpha)} = \frac{-Mg\left[x_C(\delta,\alpha) - x_S\right] f(\alpha) - \sigma f'(\alpha)\dot{\alpha}}{f^2(\alpha)}. \qquad (5.2)$$

Here instead of $\dot{\sigma}$ we used the expression $-Mg\left[x_C(\delta,\alpha) - x_S\right]$ (see (2.10)).

The derivative $\ddot{\alpha}$ (5.2) is a function of the variables α, $\dot{\alpha}$ and of the vector d, which is formed by the biped parameters and the coefficients of the polynomials (2.1). We can now substitute the polynomials (2.1) and this second derivative (5.2) in expressions (2.2) for derivatives $\ddot{\delta}_\ell$ (ℓ = 1, ..., 4). This allows us to calculate derivatives $\ddot{\delta}_\ell$ (ℓ = 1, ..., 4) as functions of variables α, $\dot{\alpha}$ and d. Then, we can substitute the expressions obtained for the derivatives $\ddot{\alpha}$ and $\ddot{\delta}_\ell$ (ℓ = 1, ..., 4) in the first four scalar equations of system (5.1). We substitute also in these four equations instead of δ, $\dot{\delta}$ expressions (2.1) – (2.3) via α and $\dot{\alpha}$. The matrix E_4 is non-singular. Therefore, the four inter-link torques seen in these four scalar equations are defined as functions of variables α, $\dot{\alpha}$ and vector d

$$\Gamma = \Gamma(\alpha, \dot{\alpha}, d) \tag{5.3}$$

So far we have not described an explicit form of control (5.3). We have only considered how to calculate the torque control at each instant in time. To implement computed torque control (5.3) we need to measure angle α and angular velocity $\dot{\alpha}$. We also need sensors to measure variables δ and $\dot{\delta}$, as they are necessary for calculating the coefficients of the polynomials (2.1) at the start of the single support phase. A further advantage of measuring variables δ and $\dot{\delta}$, is that we can design new polynomials (2.1) several times during one swing phase, each time using new polynomial coefficients to compute the control (5.3). Such an approach helps compensate for disturbances encountered by the biped during the single support phase. If measurements of variables δ, $\dot{\delta}$, α, $\dot{\alpha}$ are made at each time instant, control Γ can be calculated for each sampling period as defined above. In sum, we obtain the feedback control Γ defined in function of variables δ, $\dot{\delta}$, α, $\dot{\alpha}$.

We have shown in previous sections that biped motion designed with computed polynomials converges to a periodic regime asymptotically. When biped parameters are known perfectly, the control (5.3) (or feedback control) ensures that the bipedal motion converges to a periodic regime as well.

We also can track the reference trajectory using classical computed torque control. This torque control can be expressed by

$$\begin{aligned} \ddot{\delta} &= \ddot{\delta}(\alpha) - K_p\left[\delta - \delta(\alpha)\right] - K_v\left[\dot{\delta} - \dot{\delta}(\alpha)\right] \\ &= \delta'(\alpha)\ddot{\alpha} + \delta''(\alpha)\dot{\alpha}^2 - K_p\left[\delta - \delta(\alpha)\right] - K_v\left[\dot{\delta} - \delta'(\alpha)\dot{\alpha}\right] \end{aligned} \tag{5.4}$$

Here K_p and K_v are diagonal matrices of the feedback gains $k_{p\ell}$ and $k_{v\ell}$ $(\ell = 1, ..., 4)$, and $\delta(\alpha)$ is the vector-function 4×1 (consisting of the designed polynomials). These polynomials and function $f(\alpha)$ are computed at the start of each single support motion, and they are not modified during this motion. We substitute the second derivative $\ddot{\alpha}$ (5.2) in the expression (5.4) and in the first four scalar equations of system (5.1). Then the vector Γ of the torques can be derived from these four equations in the usual manner. The feedback gains $k_{p\ell} = 2000\ s^{-2}$ and $k_{v\ell} = 90\ s^{-1}$ $(\ell = 1, ..., 4)$ were tested in numerical experiments. In the Section 6, these experiments are presented for the case when trunk mass is known with $\pm 10\%$ of accuracy.

6. Evaluation of Acceptable Perturbations in Initial Conditions and Parameters

In this section we will partially evaluate the robustness of our method of reference trajectory design and of computed torque control (5.4).

Let us first consider cases when the initial configuration of the biped differs from the initial configuration of the periodic regime. In the periodic regime, the distance *dist* between the leg tips at the start of the single support equals *0.4248 m*. In accordance with $dist = (0.4248 \pm 0.07 \cdot 0.4248)\ m$, we will use the values *dist = 0.4545m* and *dist = 0.3951m*. For the case when *dist = 0.4545 m*, the following values of the angles are used:

$$\alpha_i = 0.2373\,,\ \delta_1(\alpha_i) = 3.0393\,,\ \delta_2(\alpha_i) = 2.7147\,,\ \delta_3(\alpha_i) = -0.5769\,,\ \delta_4(\alpha_i) = 3.0393\,. \qquad (6.1)$$

For the case when *dist = 0.3951 m*, the following values of the angles are used:

$$\alpha_i = 0.1024\,,\ \delta_1(\alpha_i) = 2.8416\,,\ \delta_2(\alpha_i) = 2.6519\,,\ \delta_3(\alpha_i) = -0.5049\,,\ \delta_4(\alpha_i) = 2.8416\,. \qquad (6.2)$$

In both cases, the reference motion converges to the periodic regime. In order to limit the number of figures, the reference trajectories are only shown for conditions (6.1) (see Fig. 15). We also tested the motions with the torso and the step length correctors, starting from initial positions (6.1) and (6.2). Applying the correctors was found to produce faster convergence to a cyclic regime.

In the three cases (using the torso corrector, the step length corrector, or no corrector at all) the acceptable errors in angular velocity $\dot{\alpha}_i$ are presented respectively by inequalities (4.8), (4.13) and (4.1). The step to step transition processes for $\dot{\alpha}_i$, with and without the correctors, are shown and compared in Fig. 11 and Fig. 14. It follows from these figures and from ***Appendix 4*** that the corresponding reference trajectories converge to periodic trajectories.

Now let us investigate cases where errors in the initial angular trunk velocity are found. In our periodic regime, the angular trunk velocity $\dot{\delta}_2(\alpha_i)$ equals $-1.1628\ s^{-1}$. We are looking at two cases: $\dot{\delta}_2(\alpha_i) = (-1.1628 \pm 1.5 \cdot 1.1628)\ s^{-1} = 0.5814\ s^{-1}, -2.9070\ s^{-1}$. In both cases, the motion converges to a periodic regime. We also tested the torso corrector and the step length corrector for both cases. The cycles with the correctors were found to converge to the nominal regime faster.

Finally, let's evaluate the robustness of the computed torque control using equations (5.4). We shall assume that torque control Γ° is computed from model (5.1) with the "nominal" trunk mass $m_3 = 20\ kg$ and the "nominal" trunk inertia moment $I_3 = 1.418\ kg \cdot m^2$ (see Appendix 1). If we allow $\pm 10\%$ variations in these values we get the following parameters, $m_3 = (20 \pm 2)kg$ and $I_3 = (1.418 \pm 0.1418)kg \cdot m^2$. Now we apply the same torque control Γ° (computed for "nominal" parameter values) in both cases. Numerical experiments, for both cases show that each error

component $\Delta\delta_\ell$ ($\ell = 1, ..., 4$) occurs less than 10^{-3} times during single support motion. Increasing gains $k_{p\ell}$ and $k_{v\ell}$ ($\ell = 1, ..., 4$), we can further decrease these errors.

7. Conclusion

We have studied a walking biped with a planar gait, which can be characterized by a swing phase and an instantaneous double support phase. In the swing phase, our footless biped has five degrees of freedom and only four drives. Thus, the system is under-actuated. The reference trajectory for each driven inter-link angle in the swing phase is described by a polynomial function of the non-driven variable of the biped, the stance leg ankle angle. If this angle changes in a strictly monotonic manner, we can use it as an independent variable instead of time. This helps us to "reduce" the number of dependent variables. Under this approach, our under-actuated system becomes like a system where the number of the actuators equals the number of degrees of freedom. This is the principal advantage of our approach relative to numerous other methods proposed in the past. Previous studies have used time in designing the reference trajectory of bipeds (*i.e.* each driven inter-link angle is given as a function of time). Because the ankle angle of the stance leg is not actuated and because disturbances may cause the swing leg to touch the ground before or after the prescribed time, configuration errors at the start of the next half step can occur. Our definition of the reference trajectory as a function of the non-driven inter-link angle eliminates this problem.

The designed nominal reference trajectory (gait) evolves to a cyclic trajectory asymptotically. The Poincaré return map method was used to generate this cyclic gait regime and show its stability. With our approach we were able to use a one-dimensional Poincaré map.

Reference trajectories are always dependent on a desired final configuration *i.e*., for example, on a final torso inclination and step length. We are able to accelerate convergence of the nominal reference gait to the cyclic gait regime by varying these two configuration parameters. In both cases we generated a correction law, where the parameter which changes is linearly dependent on its initial deviation (in the initial configuration) and on the initial deviation of the angular velocity of the supporting tibia. There is a clear relationship between our approach to cyclic gait stabilization and a biomechanical approach. Should disturbances occur while a person walking, the natural reaction is to compensate and this often means quite simply, advancing the leg a little more or less, a little faster or slower, or perhaps bending forward or backward.

Our control strategy actually has two levels of "adaptation". The goal of the first level is to speed up the convergence of the nominal reference trajectory to the cyclic trajectory. The goal of the second

level is to track the reference trajectory. We have implemented computed torque control into this tracking method. So far our control strategy has been shown to be effective tool for designing bipedal walking locomotion. In the future, we hope to use the same approach and extend it to include a non-instantaneous double support phase.

Appendix *1. Dynamic Model.*

The matrices of the dynamic model (1.1), (1.2) are shown below. The indices $i = 1$, $i = 2$ and $i = 3$ refer respectively to the shins, the femurs and the trunk. l_i equals the length of link i (i=1,2,3), m_i equals the mass of link i, I_i is the moment of inertia of link i around the axis passing through its mass center, s_i represents the distance between the mass center of link i and the corresponding joint (the hip joint for the femurs). Using these definitions we have:

$I_1 = 0.8784\ kg \cdot m^2$, $I_2 = 0.8993\ kg \cdot m^2$, $I_3 = 1.4180\ kg \cdot m^2$,

$l_1 = l_2 = 0.4\ m$, $l_3 = 0.625\ m$, $s_1 = 0.127\ m$, $s_2 = 0.163\ m$, $s_3 = 0.2\ m$,

$m_1 = 3.2\ kg$, $m_2 = 6.8\ kg$, $m_3 = 20\ kg$.

The masses of the actuators and gears are taken into account in the masses of the biped links.

The symmetric matrix $A(q)$ of the kinetic energy can be expressed as

$$A(q) = \begin{Vmatrix} 2(m_1+m_2)+m_3 & 0 & a_{13} & 2(m_1s_3+m_2s_3)\cos(-\alpha+\delta_1-\delta_2) & a_{15} & a_{16} & a_{17} \\ * & 2(m_1+m_2)+m_3 & a_{23} & a_{24} & a_{25} & a_{26} & a_{27} \\ * & * & a_{33} & a_{34} & a_{35} & a_{36} & a_{37} \\ * & * & * & I_3+2(m_2+m_1)s_3^2 & a_{45} & a_{46} & a_{47} \\ * & * & * & * & a_{55} & a_{56} & a_{57} \\ * & * & * & * & * & I_1+m_1s_1^2 & a_{67} \\ * & * & * & * & * & * & a_{77} \end{Vmatrix}$$

with

$$a_{33} = -2(m_1l_2s_3+ m_2s_2s_3)\cos(\delta_2)-2m_1l_4s_1\cos(\delta_4)-2(m_1s_3l_4+ m_2s_2s_3)\cos(\delta_3-\delta_2)$$
$$+2m_1s_1s_3\cos(\delta_3-\delta_2+\delta_4)+I_1+2I_2+ I_3+2m_2 s_2^2+2(m_1+ m_2) s_3^2 +m_1 l_2^2+m_1 l_4^2+m_1 s_1^2;$$

$$a_{55} = I_1+I_2+m_2s_2^2+m_1l_4^2+m_1s_1^2 - 2m_1l_4s_1\cos(\delta_4);$$

$$a_{77} = -2m_1l_4s_1\cos(\delta_4)-2(m_1s_3l_4+m_2s_2s_3)\cos(\delta_3-\delta_2)+2m_1s_1s_3\cos(\delta_3+\delta_4-\delta_2)$$
$$-2(m_1l_2s_3+ m_2s_2s_3)\cos(\delta_2)-2m_1l_2s_1\cos(\delta_1)+2m_1s_1s_3\cos(\delta_1-\delta_2)$$
$$+2I_1+2I_2+I_3+2m_2 s_2^2+m_1 l_4^2+2m_1 s_1^2+2m_2 s_3^2+2m_1 s_3^2+m_1 l_2^2;$$

$$a_{13} = (m_1l_4+m_2s_2)\cos(\alpha-\delta_1+\delta_3)-2(m_1s_3+m_2s_3)\cos(-\alpha+\delta_1-\delta_2)-m_1s_1\cos(\alpha-\delta_1+\delta_3+\delta_4)$$
$$+(m_2s_2+ m_1l_2)\cos(-\alpha+\delta_1);$$

$a_{15} = -(m_2 s_2 + m_1 l_4)\cos(\alpha - \delta_1 + \delta_3) + m_1 s_1 \cos(\alpha - \delta_1 + \delta_3 + \delta_4)$;

$a_{16} = m_1 s_1 \cos(\alpha - \delta_1 + \delta_3 + \delta_4)$;

$a_{17} = -(m_2 s_2 + m_1 l_4)\cos(\alpha - \delta_1 + \delta_3) + (2m_2 s_3 + 2m_1 s_3)\cos(-\alpha + \delta_1 - \delta_2) + m_1 s_1 \cos(\alpha - \delta_1 + \delta_3 + \delta_4)$

$-(m_2 s_2 + m_1 l_2)\cos(-\alpha + \delta_1) + m_1 s_1 \cos(\alpha)$;

$a_{23} = (m_2 s_2 + m_1 l_4)\sin(\alpha - \delta_1 + \delta_3) + 2(m_1 s_3 + m_2 s_3)\sin(-\alpha + \delta_1 - \delta_2) - m_1 s_1 \sin(\alpha - \delta_1 + \delta_3 + \delta_4)$

$-(m_1 l_2 + m_2 s_2)\sin(-\alpha + \delta_1)$;

$a_{24} = -2(m_1 s_3 + m_2 s_3)\sin(-\alpha + \delta_1 - \delta_2)$;

$a_{25} = -(m_1 l_4 + m_2 s_2)\sin(\alpha - \delta_1 + \delta_3) + m_1 s_1 \sin(\alpha - \delta_1 + \delta_3 + \delta_4)$;

$a_{26} = m_1 s_1 \sin(\alpha - \delta_1 + \delta_3 + \delta_4)$;

$a_{27} = -(m_2 s_2 + m_1 l_4)\sin(\alpha - \delta_1 + \delta_3) - 2(m_2 s_3 + m_1 s_3)\sin(-\alpha + \delta_1 - \delta_2) + (m_1 l_2 + m_2 s_2)\sin(-\alpha + \delta_1)$

$+m_1 s_1 \sin(\alpha - \delta_1 + \delta_3 + \delta_4) + m_1 s_1 \sin(\alpha)$;

$a_{34} = (m_1 s_3 l_4 + m_2 s_2 s_3)\cos(\delta_3 - \delta_2) - m_1 s_1 s_3 \cos(\delta_3 + \delta_4 - \delta_2) + (m_1 l_2 s_3 + m_2 s_2 s_3)\cos(\delta_2) - 2(m_1 + m_2) s_3^2 - I_3$;

$a_{35} = 2m_1 l_4 s_1 \cos(\delta_4) + (m_1 s_3 l_4 + m_2 s_2 s_3)\cos(\delta_3 - \delta_2) - m_1 s_1 s_3 \cos(\delta_3 + \delta_4 - \delta_2) - I_1 - I_2 - m_2 s_2^2 - m_1(s_1^2 + l_4^2)$;

$a_{36} = -I_1 - m_1 s_1^2 + m_1 l_4 s_1 \cos(\delta_4) - m_1 s_1 s_3 \cos(\delta_3 + \delta_4 - \delta_2)$;

$a_{37} = 2m_1 l_4 s_1 \cos(\delta_4) + 2(m_1 s_3 l_4 + m_2 s_2 s_3)\cos(\delta_3 - \delta_2) - 2m_1 s_1 s_3 \cos(\delta_3 + \delta_4 - \delta_2)$

$+2(m_1 l_2 s_3 + m_2 s_2 s_3)\cos(\delta_2) + m_1 l_2 s_1 \cos(\delta_1) - m_1 s_1 s_3 \cos(\delta_1 - \delta_2)$

$-I_1 - 2I_2 - I_3 - m_1 s_1^2 - m_1 l_4^2 - m_1 s_1^2 - 2 m_2 (s_2^2 + s_3^2) - m_1 l_2^2$;

$a_{45} = -(m_2 s_2 s_3 + m_1 s_3 l_4)\cos(\delta_3 - \delta_2) + m_1 s_1 s_3 \cos(\delta_3 + \delta_4 - \delta_2)$;

$a_{46} = m_1 s_1 s_3 \cos(\delta_3 + \delta_4 - \delta_2)$;

$a_{47} = I_3 + 2(m_1 + m_2) s_3^2 - (m_1 s_3 l_4 + m_2 s_2 s_3)\cos(\delta_3 - \delta_2) + m_1 s_1 s_3 \cos(\delta_3 + \delta_4 - \delta_2)$

$-(m_1 l_2 s_3 + m_2 s_2 s_3)\cos(\delta_2) + m_1 s_1 s_3 \cos(\delta_1 - \delta_2)$;

$a_{56} = I_1 + m_1 s_1^2 - m_1 l_4 s_1 \cos(\delta_4)$;

$a_{57} = -2m_1 l_4 s_1 \cos(\delta_4) - (m_1 s_3 l_4 + m_2 s_2 s_3)\cos(\delta_3 - \delta_2)$

$+m_1 s_1 s_3 \cos(\delta_3 + \delta_4 - \delta_2) + I_1 + I_2 + m_2 s_2^2 + m_1 l_4^2 + m_1 s_1^2$;

$a_{67} = I_1 - m_1 l_4 s_1 \cos(\delta_4) + m_1 s_1^2 + m_1 s_1 s_3 \cos(\delta_3 + \delta_4 - \delta_2)$;

$H(q, \dot{q}) = \left\| h_1,\ h_2,\ h_3,\ h_4,\ h_5,\ h_6,\ h_7 \right\|^*$

with

$h_1 = (\dot{\alpha} - \dot{\delta}_1)(m_2 s_2 + m_1 l_2) \sin(-\alpha + \delta_1) + (\dot{\delta}_1 - \dot{\delta}_3 - \dot{\alpha})^2 (m_2 s_2 + m_1 l_4) \sin(\alpha - \delta_1 + \delta_3) - m_1 s_1 \sin(\alpha)\dot{\alpha}^2$

$- m_1 s_1 (\dot{\alpha} - \dot{\delta}_1 + \dot{\delta}_3 + \dot{\delta}_4)^2 \sin(\alpha - \delta_1 + \delta_3 + \delta_4) + 2 s_3 (\dot{\alpha} - \dot{\delta}_1 + \dot{\delta}_2)^2 (m_2 + m_1) \sin(-\alpha + \delta_1 - \delta_2);$

$h_2 = -(\dot{\alpha} - \dot{\delta}_1)^2 (m_2 s_2 + m_1 l_2) \cos(-\alpha + \delta_1) - (\dot{\alpha} - \dot{\delta}_1 + \dot{\delta}_3)^2 (m_2 s_2 + m_1 l_4) \cos(\alpha - \delta_1 + \delta_3) - m_1 s_1 \cos(\alpha)\dot{\alpha}^2$

$+ m_1 s_1 (\dot{\alpha} - \dot{\delta}_1 + \dot{\delta}_3 + \dot{\delta}_4)^2 \cos(\alpha - \delta_1 + \delta_3 + \delta_4) + 2 s_3 (-\dot{\delta}_2 - \dot{\alpha} + \dot{\delta}_1)^2 (m_2 + m_1) \sin(-\alpha + \delta_1 - \delta_2);$

$h_3 = m_1 s_1 l_4 \dot{\delta}_4 (2\dot{\delta}_1 - 2\dot{\delta}_3 - \dot{\delta}_4 - 2\dot{\alpha}) \sin(\delta_4) - \dot{\delta}_2 s_3 (m_2 s_2 + m_1 l_2)(\dot{\delta}_2 + 2\dot{\alpha} - 2\dot{\delta}_1 \sin(\delta_2)$

$+ s_3 (m_1 l_4 + m_2 s_2)(\dot{\delta}_2 - \dot{\delta}_3)(\dot{\delta}_2 - 2\dot{\delta}_1 + 2\dot{\alpha} + \dot{\delta}_3) \sin(\delta_3 - \delta_2)$

$- s_3 m_1 s_1 (-\dot{\delta}_3 + \dot{\delta}_2 - \dot{\delta}_4)(\dot{\delta}_2 + 2\dot{\alpha} - 2\dot{\delta}_1 + \dot{\delta}_3 + \dot{\delta}_4) \sin(\delta_3 + \delta_4 - \delta_2)$

$- m_1 s_1 \dot{\alpha}^2 l_2 \sin(\delta_1) + m_1 s_1 s_3 \dot{\alpha}^2 \sin(\delta_1 - \delta_2);$

$h_4 = -s_3 (\dot{\delta}_1 - \dot{\alpha})^2 (s_2 m_2 + m_1 l_2) \sin(\delta_2) + s_3 (-\dot{\delta}_3 - \dot{\alpha} + \dot{\delta}_1)^2 (m_1 l_4 + s_2 m_2) \sin(\delta_3 - \delta_2)$

$- m_1 s_3 s_1 (-\dot{\delta}_4 + \dot{\delta}_1 - \dot{\delta}_3 - \dot{\alpha})^2 \sin(\delta_3 + \delta_4 - \delta_2) - s_3 \dot{\alpha}^2 m_1 s_1 \sin(\delta_1 - \delta_2);$

$h_5 = -m_1 l_4 s_1 \dot{\delta}_4 (-2\dot{\alpha} + 2\dot{\delta}_1 - 2\dot{\delta}_3 - \dot{\delta}_4) \sin(\delta_4) - s_3 (\dot{\alpha} - \dot{\delta}_1 + \dot{\delta}_2)^2 (s_2 m_2 + m_1 l_4) \sin(\delta_3 - \delta_2)$

$+ s_3 m_1 s_1 (-\dot{\delta}_2 - \dot{\alpha} + \dot{\delta}_1)^2 \sin(\delta_3 + \delta_4 - \delta_2);$

$h_6 = -m_1 s_1 l_4 (\dot{\delta}_1 - \dot{\delta}_3 - \dot{\alpha})^2 \sin(\delta_4) + m_1 s_1 s_3 (\dot{\delta}_1 - \dot{\delta}_2 - \dot{\alpha})^2 \sin(\delta_3 + \delta_4 - \delta_2);$

$h_7 = -m_1 l_4 s_1 \dot{\delta}_4 (-\dot{\delta}_4 + 2\dot{\delta}_1 - 2\dot{\alpha} - 2\dot{\delta}_3) \sin(\delta_4) - s_3 (m_2 s_2 + m_1 l_2)\ \dot{\delta}_2 (-\dot{\delta}_2 - 2\dot{\alpha} + 2\dot{\delta}_1) \sin(\delta_2)$

$- (-\dot{\delta}_3 + \dot{\delta}_2)(\dot{\delta}_2 - 2\dot{\delta}_1 + 2\dot{\alpha} + \dot{\delta}_3)(m_1 l_4 + s_2 m_2)\ s_3 \sin(\delta_3 - \delta_2)$

$+ m_1 l_2 s_1 \dot{\delta}_1 (-\dot{\delta}_1 + 2\dot{\alpha}) \sin(\delta_1) + m_1 s_3 s_1 (\dot{\delta}_1 - \dot{\delta}_2)(\dot{\delta}_1 - \dot{\delta}_2 - 2\dot{\alpha}) \sin(\delta_1 - \delta_2)$

$- m_1 s_3 s_1 (\dot{\delta}_2 - \dot{\delta}_4 - \dot{\delta}_3)(-\dot{\delta}_2 - 2\dot{\alpha} + 2\dot{\delta}_1 - \dot{\delta}_3 - \dot{\delta}_4) \sin(\delta_3 + \delta_4 - \delta_2);$

$$D = \begin{Vmatrix} 0 & 0 & 0 & 0 \\ 0 & 0 & 0 & 0 \\ 1 & 0 & 0 & 0 \\ 0 & 1 & 0 & 0 \\ 0 & 0 & 1 & 0 \\ 0 & 0 & 0 & 1 \\ 0 & 0 & 0 & 0 \end{Vmatrix};\quad D_1(q) = \begin{Vmatrix} 1 & 0 \\ 0 & 1 \\ d_{1_{31}} & d_{1_{32}} \\ d_{1_{41}} & d_{1_{42}} \\ 0 & 0 \\ 0 & 0 \\ d_{1_{71}} & d_{1_{72}} \end{Vmatrix};\quad D_2(q) = \begin{Vmatrix} 1 & 0 \\ 0 & 1 \\ d_{2_{31}} & d_{2_{32}} \\ d_{2_{41}} & d_{2_{42}} \\ d_{2_{51}} & d_{2_{52}} \\ d_{2_{61}} & d_{2_{62}} \\ d_{2_{71}} & d_{2_{72}} \end{Vmatrix};$$

with

$d_{1_{31}} = l_2 \cos(-\alpha + \delta_1) - s_3 \cos(-\alpha + \delta_1 - \delta_2);\ d_{1_{32}} = -l_2 \sin(-\alpha + \delta_1) + s_3 \sin(-\alpha + \delta_1 - \delta_2);$

$d_{1_{41}} = s_3 \cos(-\alpha + \delta_1 - \delta_2);\ d_{1_{42}} = -s_3 \sin(-\alpha + \delta_1 - \delta_2);$

$d_{1_{71}} = l_1 \cos(\alpha) - l_2 \cos(-\alpha + \delta_1) + s_3 \cos(-\alpha + \delta_1 - \delta_2);\ d_{1_{72}} = l_1 \sin(\alpha) + l_2 \sin(-\alpha + \delta_1) - s_3 \sin(-\alpha + \delta_1 - \delta_2);$

$d_{2_{31}} = -l_5\cos(\alpha-\delta_1+\delta_3+\delta_4)+l_4\cos(\alpha-\delta_1+\delta_3)-s_3\cos(-\alpha+\delta_1-\delta_2)$;

$d_{2_{32}} = -l_5\sin(\alpha-\delta_1+\delta_3+\delta_4)+l_4\sin(\alpha-\delta_1+\delta_3)+s_3\sin(-\alpha+\delta_1-\delta_2)$;

$d_{2_{41}}=s_3\cos(-\alpha+\delta_1-\delta_2)$; $d_{2_{42}} = -s_3\sin(-\alpha+\delta_1-\delta_2)$;

$d_{2_{51}}=l_5\cos(\alpha-\delta_1+\delta_3+\delta_4)-l_4\cos(\alpha-\delta_1+\delta_3)$; $d_{2_{52}}=l_5\sin(\alpha-\delta_1+\delta_3+\delta_4)-l_4\sin(\alpha-\delta_1+\delta_3)$;

$d_{2_{61}}=l_5\cos(\alpha-\delta_1+\delta_3+\delta_4)$; $d_{2_{62}}=l_5\sin(\alpha-\delta_1+\delta_3+\delta_4)$;

$d_{2_{71}} = l_5\cos(\alpha-\delta_1+\delta_3+\delta_4)-l_4\cos(\alpha-\delta_1+\delta_3)+s_3\cos(-\alpha+\delta_1-\delta_2)$;

$d_{2_{72}} = l_5\sin(\alpha-\delta_1+\delta_3+\delta_4)-l_4\sin(\alpha-\delta_1+\delta_3)-s_3\sin(-\alpha+\delta_1-\delta_2)$;

$$H_1(q,\dot{q})\left\|\begin{array}{l} -l_2(\dot{\delta}_1-\dot{\alpha})^2\sin(-\alpha+\delta_1)+s_3(\dot{\alpha}-\dot{\delta}_1+\dot{\delta}_2)^2\sin(-\alpha+\delta_1-\delta_2)-l_1\dot{\alpha}^2\sin(\alpha) \\ -l_2(\dot{\delta}_1-\dot{\alpha})^2\sin(-\alpha+\delta_1)+s_3(\dot{\alpha}-\dot{\delta}_1+\dot{\delta}_2)^2\cos(-\alpha+\delta_1-\delta_2)+l_1\dot{\alpha}^2\cos(\alpha) \end{array}\right\|$$

$$H_2(q,\dot{q})\left\|\begin{array}{l} l_4(\dot{\alpha}-\dot{\delta}_1+\dot{\delta}_3)^2\sin(\alpha-\delta_1+\delta_3)-l_5(\dot{\alpha}-\dot{\delta}_1+\dot{\delta}_3+\dot{\delta}_4)^2\sin(\alpha-\delta_1+\delta_3+\delta_4) \\ +s_3(\dot{\alpha}-\dot{\delta}_1+\dot{\delta}_2)^2)\sin(-\alpha+\delta_1-\delta_2) \\ \\ -l4(-\dot{\delta}_3-\dot{\alpha}+\dot{\delta}_1)^2\cos(\alpha-\delta_1+\delta_3)+l_5(\dot{\alpha}-\dot{\delta}_1+\dot{\delta}_3+\dot{\delta}_4)^2\cos(\alpha-\delta_1+\delta_3+\delta_4) \\ +s_3(\dot{\alpha}-\dot{\delta}_1+\dot{\delta}_2)^2\cos(-\alpha+\delta_1-\delta_2) \end{array}\right\|$$

Appendix *2. Uniqueness of the solution of the system* (1.3)**,** (1.5).

If we consider only the two first lines of matrices $D_k(q)$ *(k=1, 2)* (see Appendix *1*), it is apparent that the columns of each matrix $D_k(q)$ are linearly independent for any configuration *q*.

Eqs. (1.3), (1.5) can be rewritten in the following form:

$$A(q(T))\dot{X}^+ - D_k(q(T))I_{R_k} = A(q(T))\dot{X}^- \qquad D_k^*(q(T))\dot{X}^+ = 0$$

The matrix of this linear system is given by

$$M(q(T)) = \left\|\begin{array}{cc} A(q(T)) & -D_k(q(T)) \\ D_k^*(q(T)) & 0 \end{array}\right\|$$

The determinant of this matrix *M(q)* can be easily calculated [31]

$$det\, M(q) = det\left\|\begin{array}{cc} A(q) & -D_k(q) \\ D_k^*(q) & 0 \end{array}\right\| = det\, A(q)\, det\left[D_k^*(q)A^{-1}(q)D_k(q)\right]$$

The symmetrical matrix *A(q)* is positive definite: *A(q)>0*. Therefore, it is non-singular. The (2×2) matrix $D_k^*(q)A^{-1}(q)D_k(q) > 0$ as well, because $A^{-1}(q) > 0$ and because the columns of matrix $D_j(q)$ are linearly independent. As a result we can deduce that $det\, M(q) \neq 0$ for any configuration *q*.

Appendix *3*. G*round reaction* $I_{R_{yk}}$ *is positive*

We can find vector $\dot{X}^+$ from equation (1.3)

$$\dot{X}^+ = A^{-1}(q)D_k(q)I_{R_k} + \dot{X}^-$$

We shall substitute the variable *q* for *q(T)*, thus equation (1.5) can be expressed as:

$$D_k^*(q)A^{-1}(q)D_k(q)I_{R_k} = -D_k^*(q)\dot{X}^-$$

It follows here from that

$$I_{R_k} = \left[D_k^*(q)A^{-1}(q)D_k(q)\right]^{-1}\left[-D_k^*(q)\dot{X}^-\right]$$

Matrix $D_k^*(q)A^{-1}(q)D_k(q) > 0$ (see Appendix 2), consequently $\left[D_k^*(q)A^{-1}(q)D_k(q)\right]^{-1} > 0$ as well. The first element of the (2×1) matrix-column $D_k^*(q)\dot{X}^-$ is the horizontal component of the fore leg tip velocity; the second element of this column is the vertical component of this velocity. We can thus see that when the fore leg tip velocity is directed exactly downwards, the first element will equal zero and the second element will be negative. From this relationship we can state that $I_{R_{yk}} > 0$.

Appendix *4*. Stability of the cyclic motion.

Let us assume that every solution of system (2.9), (2.11) (for given values (2.5) and conditions (2.4)) depends continuously on velocity $\dot{\alpha}_i$ and time *t* in some neighborhood of the nominal velocity u_e. The coefficients of the polynomials (2.1) are also continuously dependent on this velocity. Therefore, a solution $X(\dot{\alpha}_i, t)$ of the system (1.1), (1.2) is a continuous function of the velocity $\dot{\alpha}_i$ and time *t* for this neighborhood of the nominal velocity. The ordinate *y* of the swing leg tip is a continuous function, $y = y(\dot{\alpha}_i, t)$, of velocity $\dot{\alpha}_i$ and time *t* as well. It is clear that $y(u_e, T_e) = 0$. Consider now the following equation

$$y(\dot{\alpha}_i, T) = 0 \qquad (**)$$

Here *T* is the time, when the swing leg tip hits the ground. Assume that there are both continuous partial derivatives $\partial y/\partial\dot{\alpha}_i$ and $\partial y/\partial T$ in the neighborhood of the point u_e, T_e. The vector of the swing leg tip velocity is directed strictly downwards just before the instant T_e (this vector is not tangential to the ground surface). This means that $\partial y/\partial T < 0$ for $\dot{\alpha}_i = u_e$, $T = T_e$. Using the well-known implicit function theorem, we conclude from (**) that in a neighborhood of the point u_e, T_e, the continuous function $T = T(\dot{\alpha}_i)$ exists such that $T_e = T(u_e)$. Finally, if $\dot{\alpha}_i \to u_e$, then $T(\dot{\alpha}_i) \to T_e$ and

$X(\dot{\alpha}_i, t) \to X(u_e, t)$ uniformly for any time t. Thus we can affirm that the cyclic motion is asymptotically orbitally stable.

References

1. *Gubina F., Hemami H., McGhee R.B.* On the Dynamic Stability of Biped Locomotion // IEEE Trans. Biomedical Engineering. 1974. V. 21. № 2.
2. *Beletskii V.V., Chudinov P.S.* Parametric Optimization in the Problem of Bipedal Locomotion // Izv. AN SSSR. Mekhanika Tverdogo Tela [Mechanics of Solids]. 1977. № 1.
3. *Formal'sky A.M.* Locomotion of Anthropomorphic Mechanisms. Moscow. Nauka. 1982. In Russian.
4. *Katoh R., Mori M.* Control Method of Biped Locomotion Giving Asymptotic Stability of Trajectory // Automatica. 1984. V. 20. № 4.
5. *Miura H., Shimoyama I.* Dynamic Walk of a Biped // Int. J. of Robotics Research, 1984. V. 3. № 2.
6. *Raibert M.H.* Legged Robots that Balance. MIT Press, Cambridge, MA. 1986.
7. *McGeer T.* Passive Dynamic Walking // Int. J. of Robotics Research. 1990. V. 9. № 2.
8. *Sano A., Furusho J.* Realization of Natural Dynamic Walking Using the Angular Momentum Information // Proc. of IEEE Conf. on Robotics and Automation. Cincinnati, Ohio. 1990. V. 3.
9. *Vukobratovic M., Borovac B., Surla D., Stokic D.* Biped Locomotion. Scientific Fundamentals of Robotics, V. 7. Springer-Verlag. 1990.
10. *Koditschek D.D., Buhler M.* Analysis of a Simplified Hopping Robot // Int. J. of Robotics Research. 1991. V. 10. № 6.
11. *Raibert M.H., Tzafestas S., Tzafestas C.* Comparative Simulation Study of Three Control Techniques Applied to a Biped Robot // Proc. of IEEE Conf. on Systems, Man and Cybernetics, Systems Engineering in the Service of Humans. Le Touquet, France. 1993.

12. *Cheng M.-Y., Lin C.-S.* Measurement of Robustness for Biped Locomotion Using a Linearized Poincaré Map // Robotica. 1996. V. 14.

13. *Formal'sky A.M.* Ballistic Locomotion of a Biped. Design and Control of Two Biped Machines // In: Human and Machine Locomotion, ed. A.Morecki and K.Waldron. Udine, Italy: CISM, Springer-Verlag. 1997.

14. *Hirai K., Hirose M., Haikava, Y., Takenaka T.* The Development of Honda Humanoid Robot // Proc. of IEEE Conf. on Robotics and Automation. Leuven, Belgium. 1998.

15. *Kajita S., Tani K.* Experimental Study of Biped Dynamic Walking in the Linear Inverted Pendulum Mode // Proc. of IEEE Conf. on Robotics and Automation. Leuven, Belgium. 1998. V. 3.

16. *Pratt J., Pratt G.* Intuitive Control of a Planar Bipedal Walking Robot // Proc. of IEEE Conf. on Robotics and Automation. Leuven, Belgium. 1998. V. 3.

17. *Chevallereau C., Formal'sky A.M., Perrin B.* Low Energy Cost Reference Trajectories for a Biped Robot // Proc. of IEEE Conf. on Robotics and Automation. Leuven, Belgium. 1998. V. 2.

18. *Pratt J., Chew C.M., Torres A., Dilworth P., Pratt G.* Virtual Model Control: An Intuitive Approach for Bipedal Locomotion // Int. J. of Robotics Research. 2001. V. 20. № 2.

19. *Grishin A.A., Formal'sky A.M., Lensky A.V., Zhitomirsky S.V.* Dynamic Walking of Two Biped Vehicles // Proc. of 9 th World Congress on the Theory of Machines and Mechanisms. Italy. 1995. V. 3.

20. *Goswami A., Espiau B., Keramane A.V.* Limit Cycles and their Stability in a Passive Bipedal Gait // Proc. of IEEE Conf. on Robotics and Automation. Minneapolis, Minnesota. 1996. V. 1

21. *Chevallereau C., Sardain P.* Design and Actuation Optimization of a 4 Axes Biped Robot for Walking and Running // Proc. of IEEE Conf. on Robotics and Automation. San Francisco, California. 2000. V. 4.

22. *Aoustin Y., Formal'sky A*. Stability of a Cyclic Biped Gait and Hastening of the Convergence to It //Proc. of 4th CLAWAR, Karlsruhe, Germany. 2001. pp.779-788,

23. *Chevallereau C., Aoustin Y.* Optimal Reference Trajectories for Walking and Running of a Biped Robot // Robotica. 2001. V. 19.

24. *Grizzle J.W., Abba G., Plestan F.* Asymptotically Stable Walking for Biped Robots: Analysis via System with Impulse Effects // IEEE Trans. Autom. Control. 2001. V. 46. № 1.

25. *Rostami M., Bessonnet G.* Saggital Gait of a Biped Robot During the Single Support Phase. Part 1: Passive Motion // Robotica. 2001. V 19.

26. *Rostami M., Bessonnet G.* Saggital Gait of a Biped Robot During the Single Support Phase. Part 2: Optimal Motion // Robotica. 2001. V. 19.

27. *Chevallereau, C., Formal'sky A.* Suivi Géométrique d'une Trajectoire Articulaire pour la Marche d'un Bipède // Prepr. of CIFA Congress. Nantes, France. 2002.

28. *Chevallereau C.* Parametrised Control for an Underactuated Biped Robot // Prepr. of the 15th Triennial World Congress. Barcelona, Spain. 2002.

29. *Slotine J.J.E., Li W.* Applied Nonlinear Control. Prentice–Hall, Englewood Cliffs, New Jersey. 1991.

30. *Poincaré H.* Oeuvres complètes. Vol. 11. Cauthier-Villars Paris 1916-1954, réimpression Jacques Gabay, Paris. 1987-1997.

31. *Lefschetz S.* Stability of Nonlinear Control Systems. Academic Press. New York-London. 1965.

List of captions

Fig. 1. The biped.

Fig. 2. The biped's given initial, intermediate and final configurations.

Fig. 3. Non-actuated ankle angle $\alpha(t)$ for the periodic gait.

Fig. 4. Actuated joint angles $\delta_\ell(\alpha)$ ($\ell = 1, ..., 4$) for the periodic regime.

Fig. 5. Actuated joint angles $\delta_\ell(t)$ ($\ell = 1, ..., 4$) for the periodic gait.

Fig. 6. Graph of periodic walking as a sequence of stick figures.

Fig. 7. The periodic gait in planes (α,σ) and $(\psi, \dot{\psi})$.

Fig. 8. The Poincaré return map $u_{n+1} = p(u_n)$ (3.4).

Fig. 9. Function $u_{n+1} = q(u_e, v_{n-1}, v_e)$.

Fig. 10. Function $u_{n+1} = q(u_e, v_e, v_n)$.

Fig. 11. Transitional processes in plane (n, u_n) with and without torso orientation correction.

Fig. 12. Function $u_{n+1} = r(u_e, w_{n-1}, w_e)$.

Fig. 13. Function $u_{n+1} = r(u_e, w_e, w_n)$.

Fig. 14. Transitional processes in plane (n, u_n) with and without step length correction.

Fig. 15. Graphs of joint angles $\delta_\ell(t)$ ($\ell = 1, ..., 4$) under conditions (6.1) without a corrector.

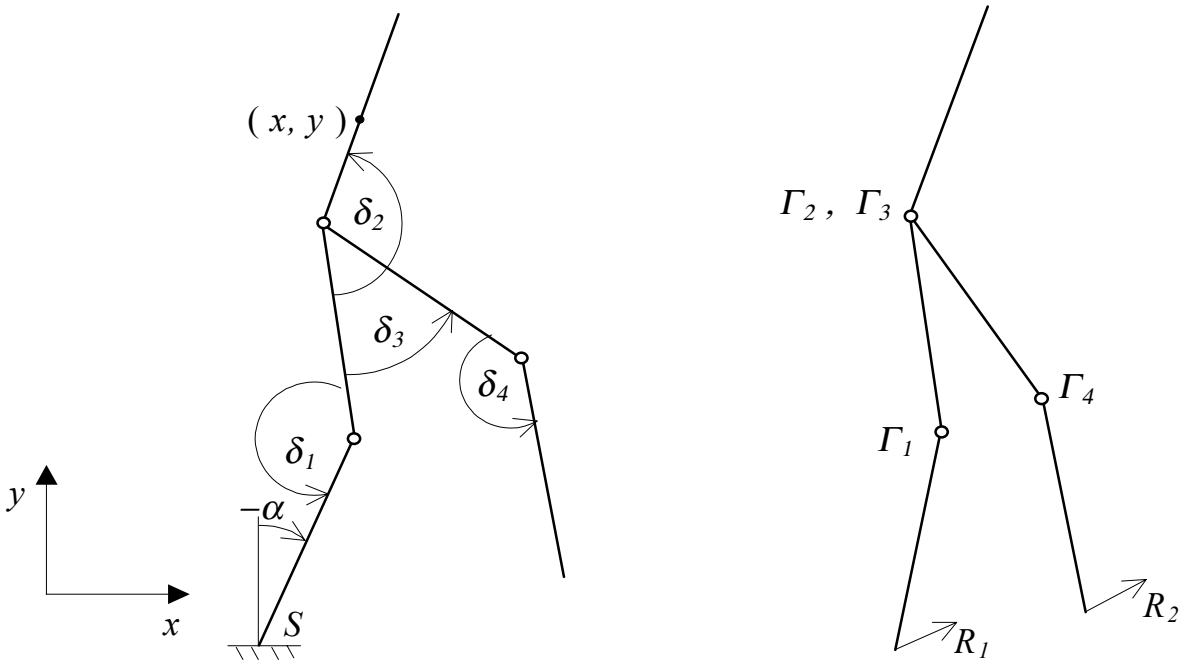

Fig. 1. The biped

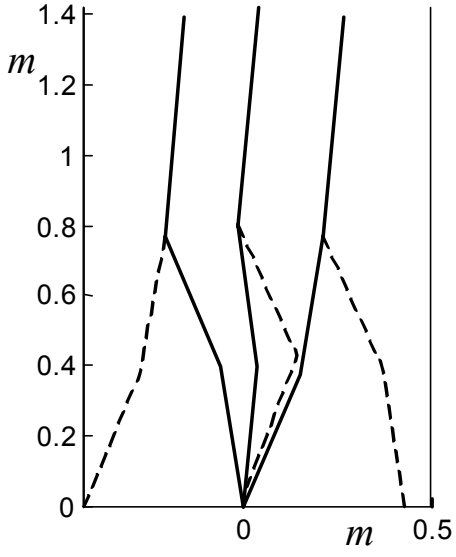

Fig. 2. The biped's given initial, intermediate and final configurations.

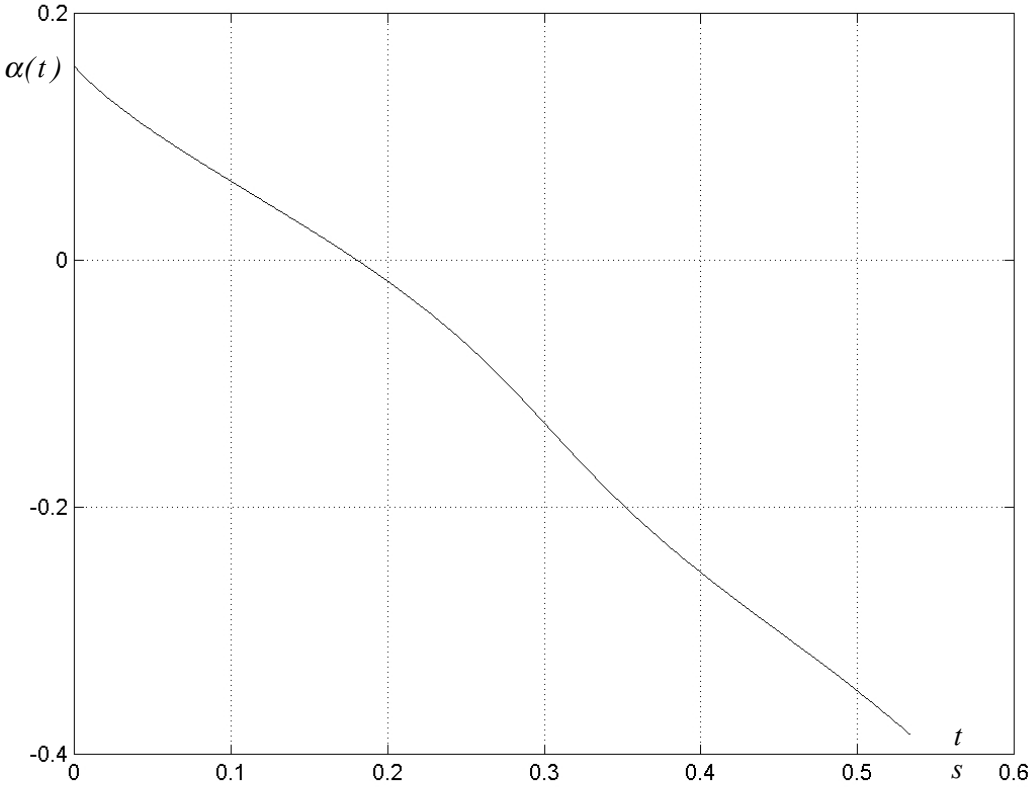

Fig. 3. Non-actuated ankle angle $\alpha(t)$ for the periodic gait.

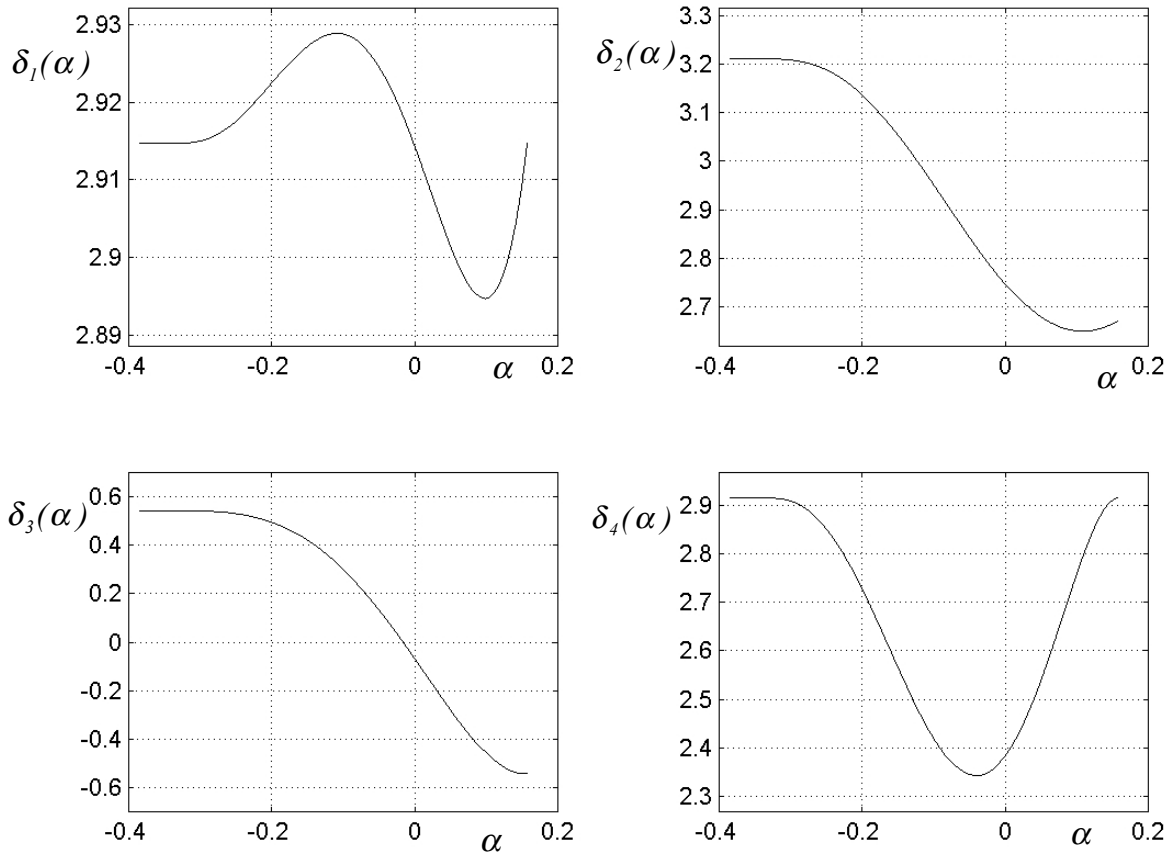

Fig. 4. Actuated joint angles $\delta_\ell(\alpha)$ ($\ell = 1, ..., 4$) for the periodic gait.

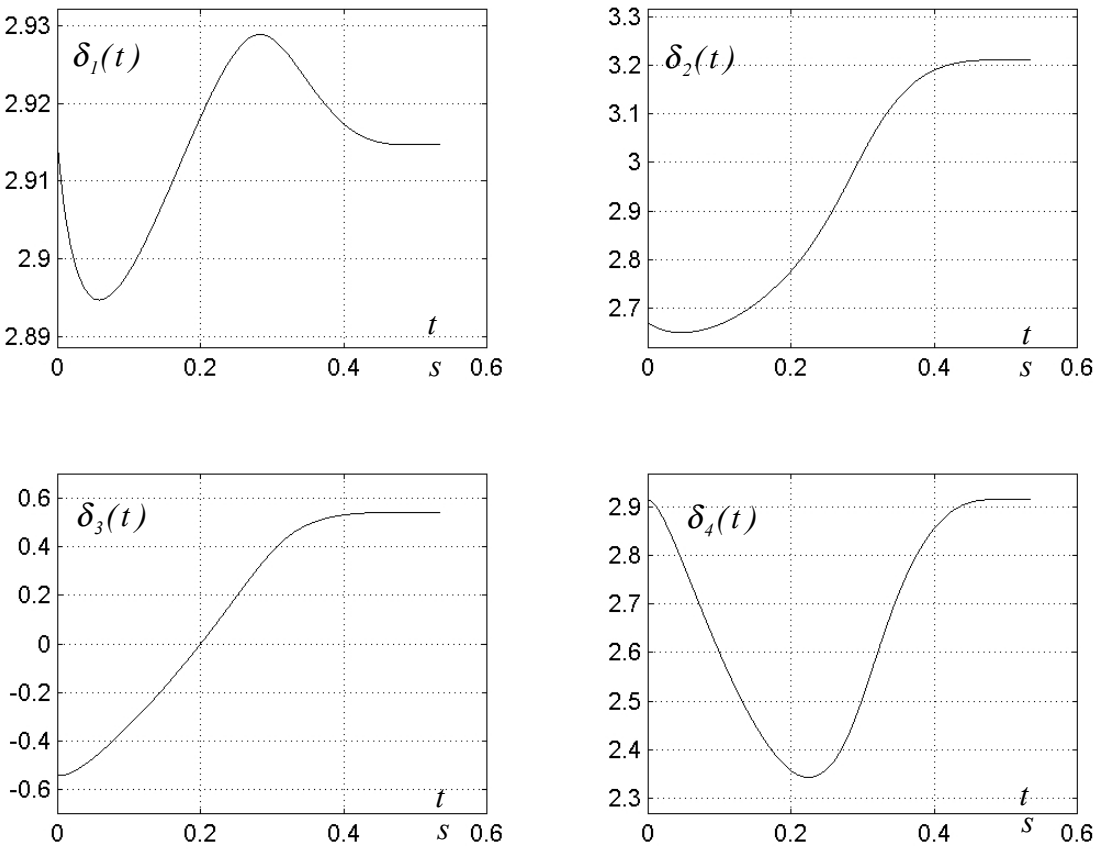

Fig. 5. Actuated joint angles $\delta_\ell(t)$ $(\ell = 1, ...,4)$ for the periodic gait.

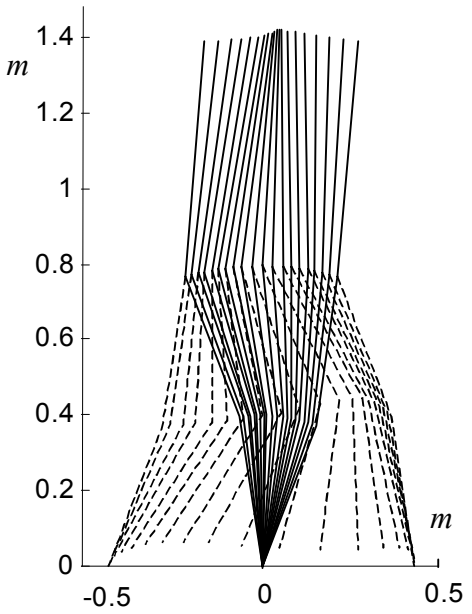

Fig. 6. Graph of periodic walking as a sequence of stick figures.

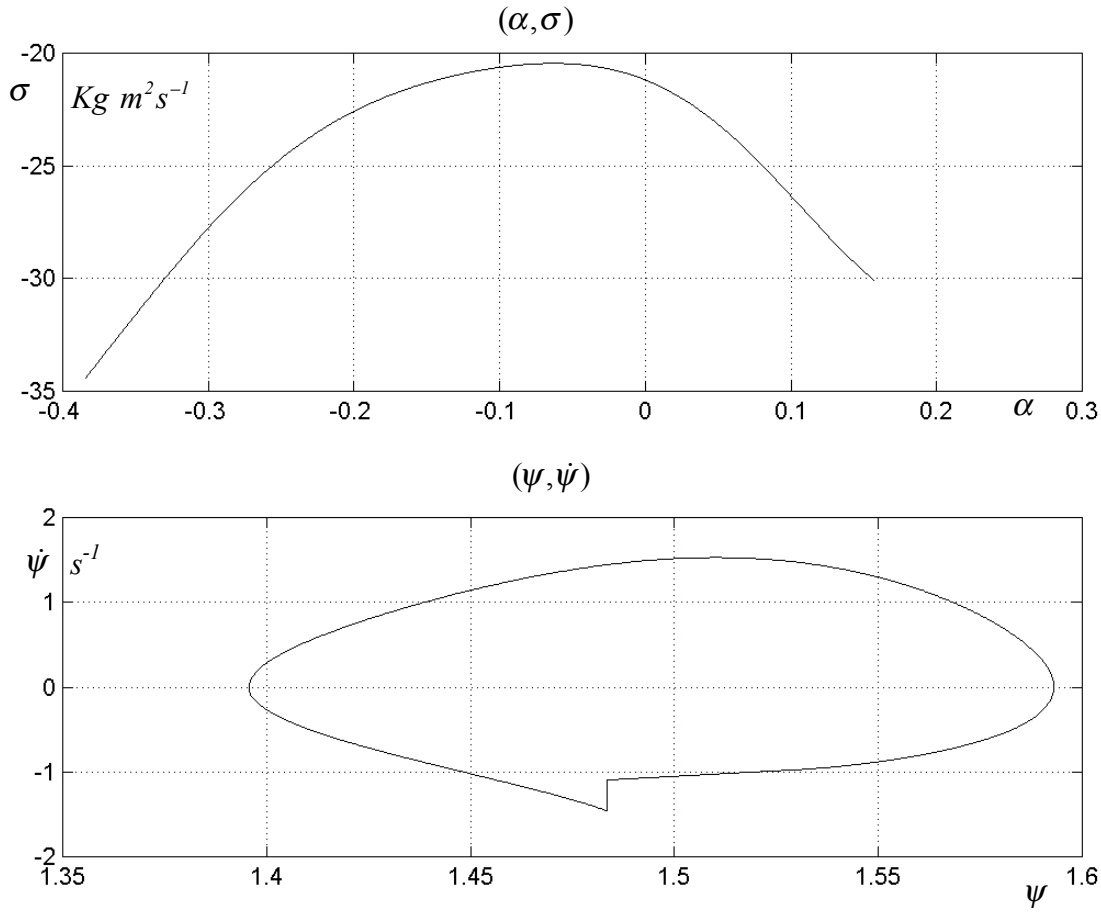

Fig. 7. The periodic gait in planes (α,σ) and $(\psi,\ \dot{\psi})$.

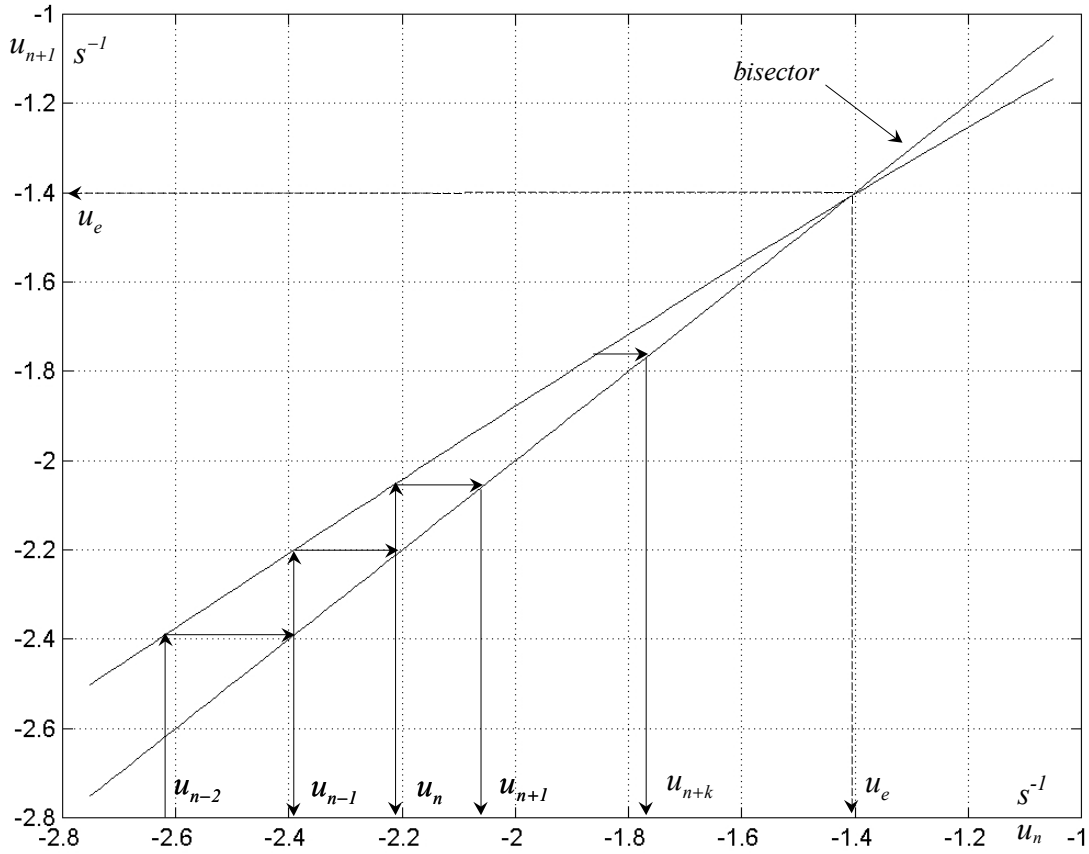

Fig. 8. The Poincaré return map $u_{n+1} = p(u_n)$ (3.4).

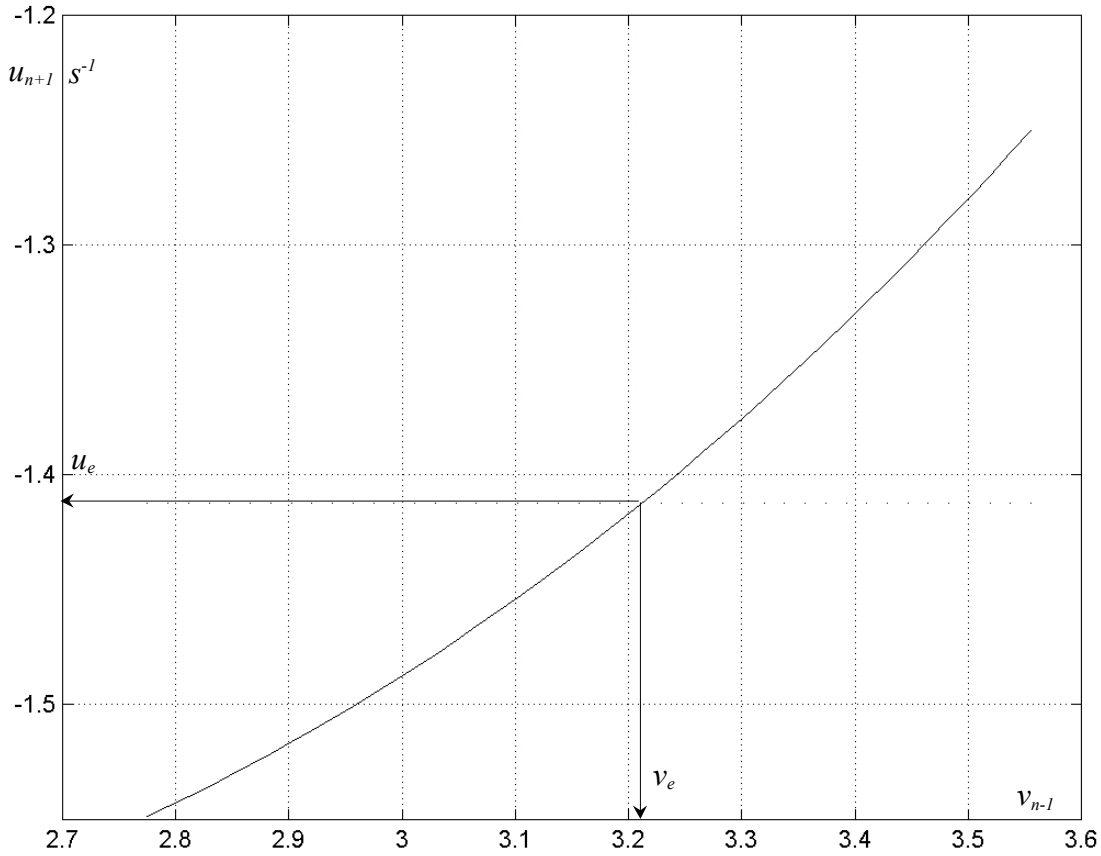

Fig. 9. Function $u_{n+1} = q(u_e,\ v_{n-1},\ v_e)$.

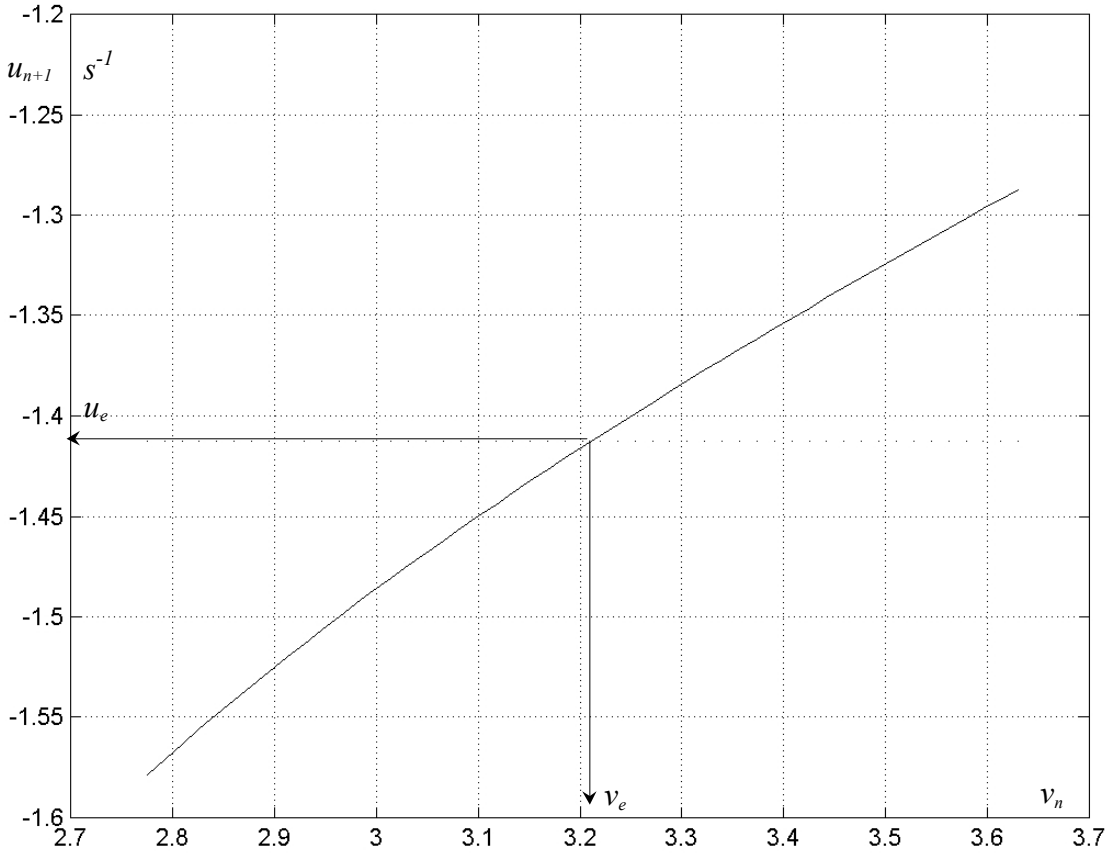

Fig. 10. Function $u_{n+1} = q(u_e, v_e, v_n)$.

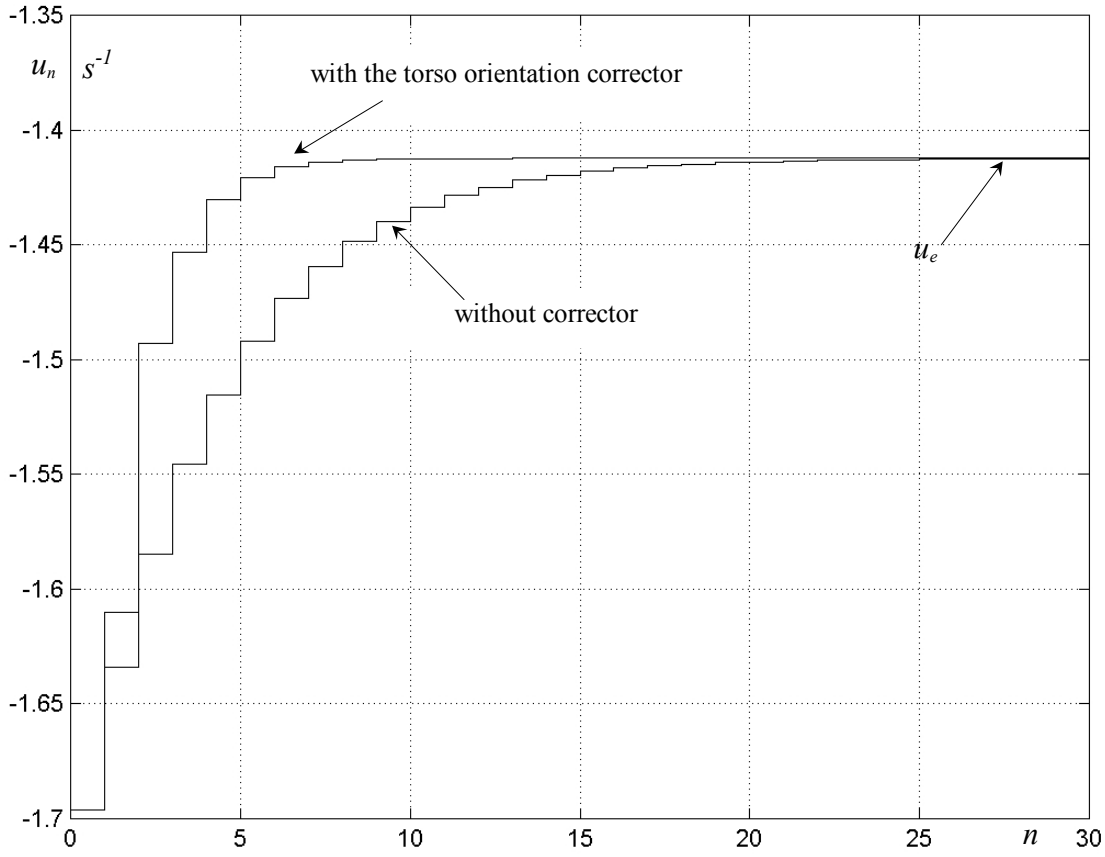

Fig. 11. Transitional processes in plane (n, u_n) with and without torso orientation correction.

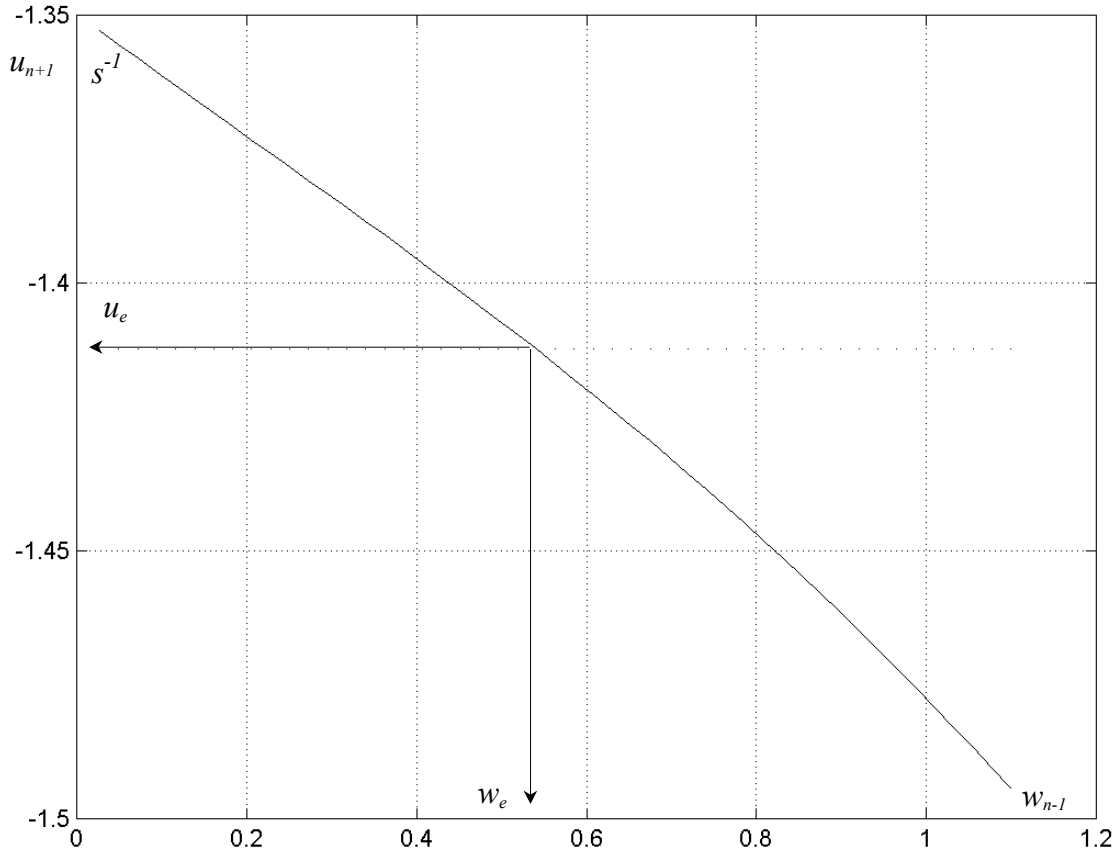

Fig. 12. Function $u_{n+1} = r(u_e,\ w_{n-1},\ w_e)$.

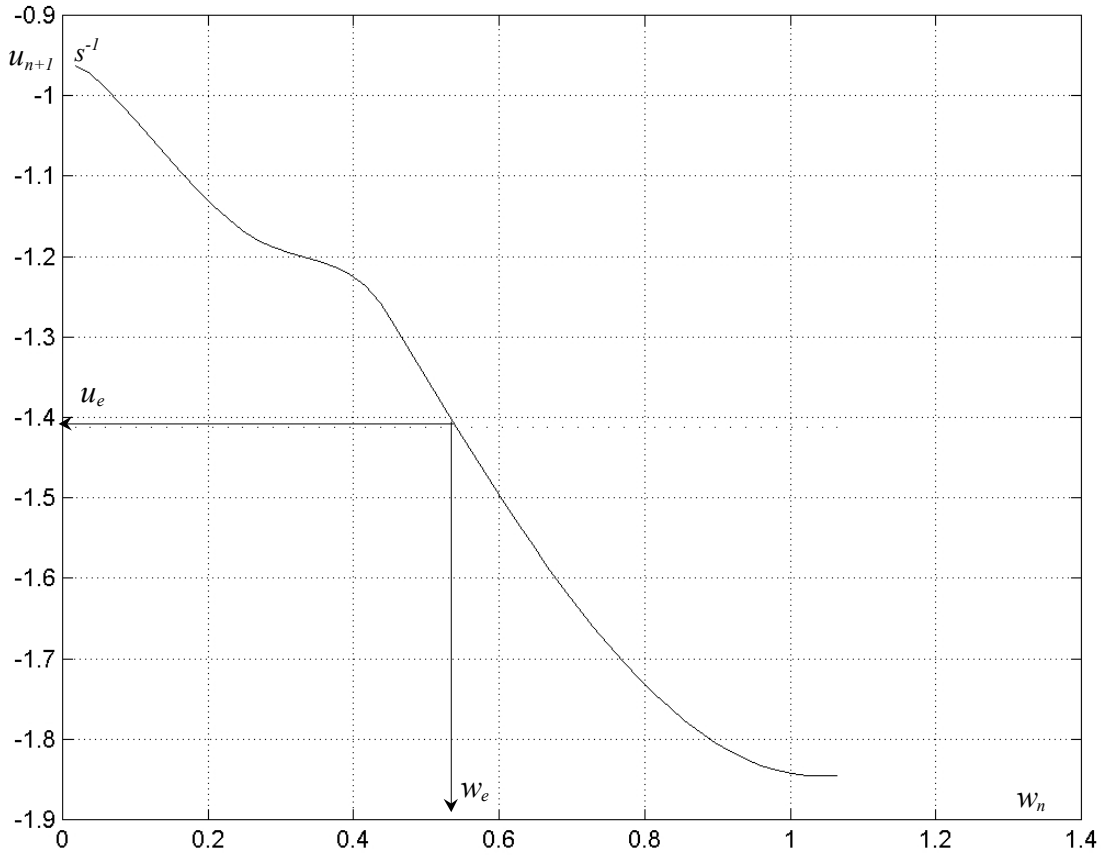

Fig. 13. Function $u_{n+1} = r(u_e, w_e, w_n)$.

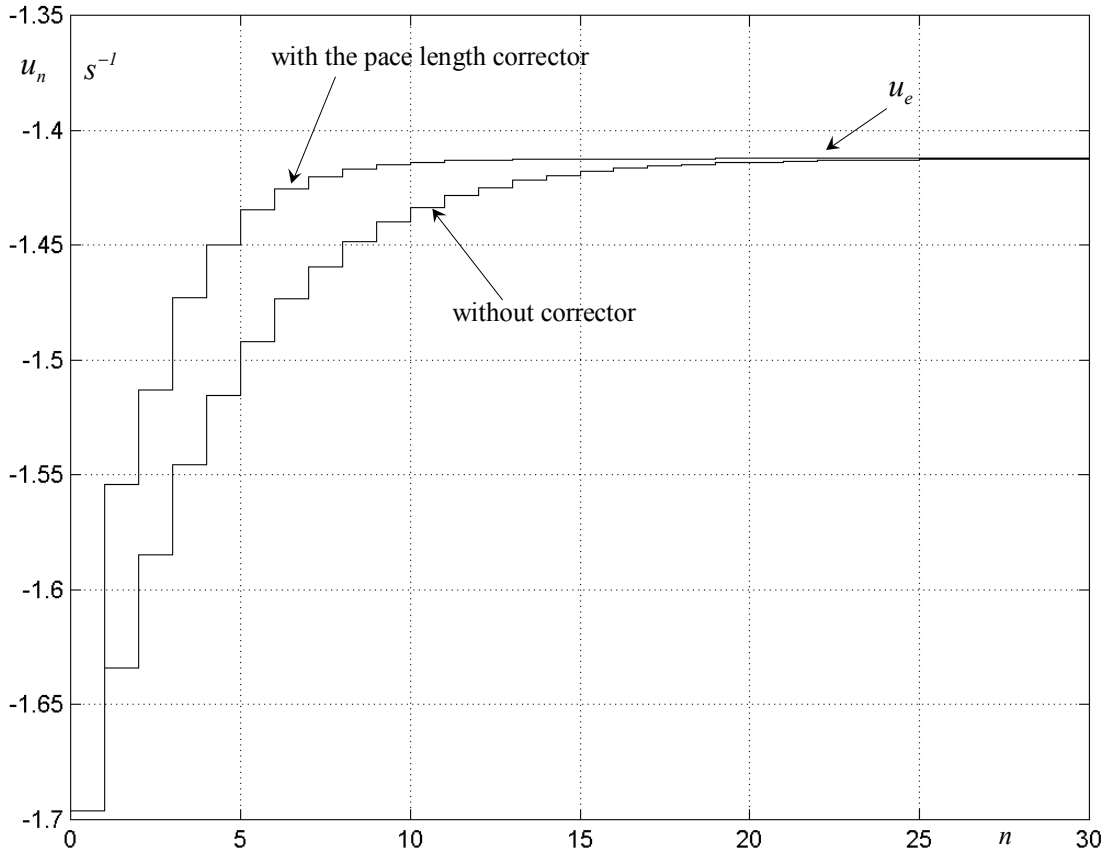

Fig. 14. Transitional processes in plane (n, u_n) with and without step length correction.

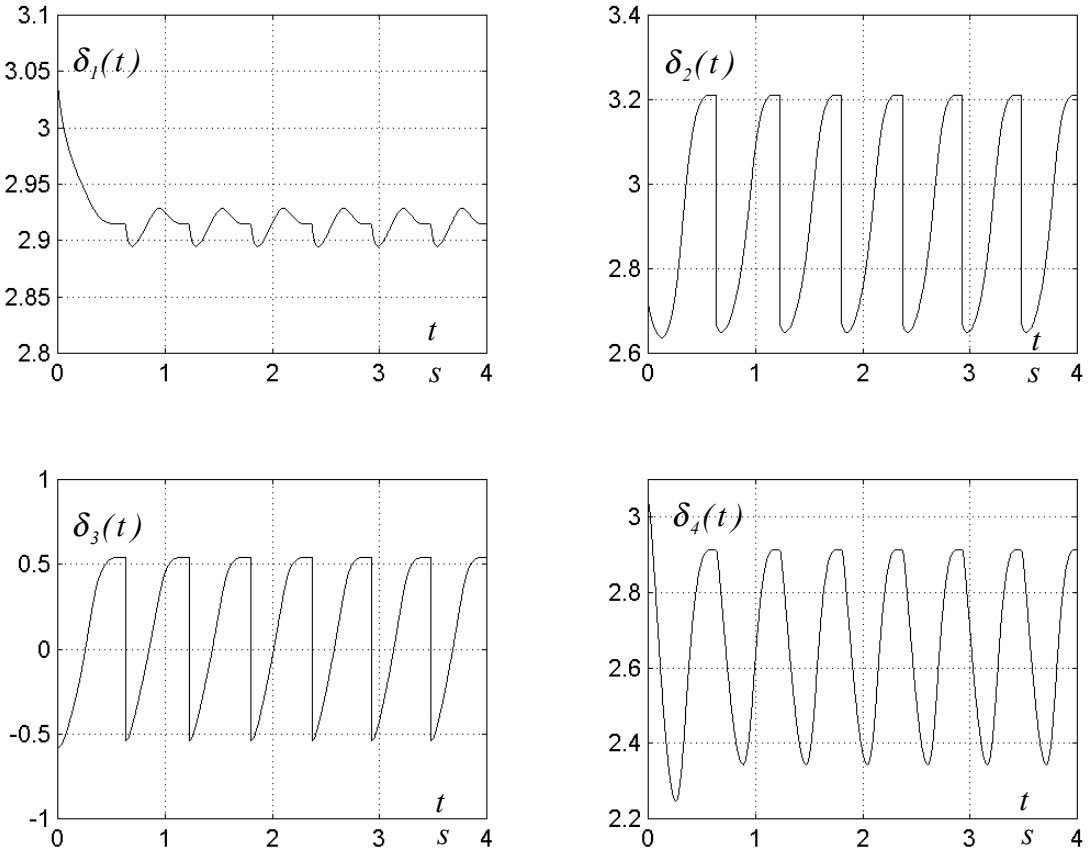

Fig. 15. Graphs of joint angles $\delta_\ell(t)$ ($\ell = 1, ..., 4$) under conditions (6.1) without a corrector.